Improving rice drought tolerance through host-mediated microbiome selection

Alex Styer[1,2], Dean Pettinga[1,2], Daniel Caddell[1,2], Devin Coleman-Derr[1,2]

[1] Department of Plant and Microbial Biology, 111 Koshland Hall, University of California, Berkeley, CA, USA

[2] Plant Gene Expression Center, USDA-ARS, Albany, CA, USA

Abstract

Plant microbiome engineering remains a significant challenge due to challenges associated with accurately predicting microbiome assembly and function in complex, heterogeneous soil environments. However, host-mediated selection can simplify the process by using plant host phenotype as a reporter of microbiome function; by iteratively selecting microbiomes from hosts with desired phenotypes and using them to inoculate subsequent cohorts of hosts, artificial selection can steer the microbiome towards a composition producing optimized plant phenotypes. In this study, we inoculated rice with wild microbial communities from fallow rice field, desert, and serpentine seep field soils. By challenging these plants with drought and iteratively selecting microbiomes from the least drought stressed plants across multiple generations, we derived simplified microbiomes that enhanced both the growth and drought tolerance of rice. Across selection cycles, microbiomes within and between soil treatments became increasingly similar, implicating both dispersal and selection as drivers of community composition. With amplicon sequencing data we identified specific bacterial taxa associated with improved rice drought phenotypes; while many of these taxa have been previously described as plant growth promoters, we also identified novel taxa exhibiting strong positive correlation with improved drought performance. Lastly, we resolved 272 metagenome-assembled genomes (MAGs) and used these MAGs to identify functions enriched in bacteria driving enhanced drought tolerance. The most significantly enriched functions—particularly glycerol-3-phosphate and iron transport—have been previously implicated as potential mediators of plant-microbe interactions during drought. Altogether, these data demonstrate that host-mediated selection provides an efficient framework for microbiome engineering through the identification of both individual taxa and simplified communities associated with enhanced plant phenotypes.

Introduction

Plant-associated microbiota directly affect the fitness of their hosts through a variety of mechanisms. These mechanisms include interactions with plant immunity (Pieterse et al. 2014; Durrant and Dong 2004; Schlatter et al. 2017), secretion and metabolism of phytohormones and other signaling molecules (Orozco-Mosqueda, Santoyo, and Glick 2023; Spaepen 2015; Spaepen and Vanderleyden 2011; Glick 2005), mediating nutrient bioavailability (P. Xu and Wang 2023; Richardson and Simpson 2011; Kramer, Özkaya, and Kümmerli 2020), and

otherwise altering the physico-chemical environment experienced by plants (Liu et al. 2020; Kumar et al. 2020). Intentional manipulation of plant microbiomes to enhance fitness—through growth promotion, disease suppression, and alleviation of abiotic stress—therefore represents an alternative or supplement to plant breeding to improve agricultural productivity (Friesen et al. 2011; Finkel et al. 2017; Shayanthan, Ordoñez, and Oresnik 2022; Vorholt et al. 2017).

Many individual bacterial and fungal isolates have already been proven capable of plant growth promotion in lab studies (Rodrigues et al. 2008; Bilal et al. 2018; Fan and Smith 2022; Karmakar et al. 2021; Franche, Lindström, and Elmerich 2009), but they often fail to perform similarly well in the field (Sessitsch, Pfaffenbichler, and Mitter 2019). The proximate cause for the performance gap is usually poor colonization and survival (Albareda, Rodríguez-Navarro, and Temprano 2009), but ultimately the discrepancy lies in the difficulty of screening isolates in ways that recapitulate field environments (Russ et al. 2023). In other words, because the strength and direction of a microbe or synthetic community's (syncom) effect on plant fitness emerge from complex interactions between—and among—plants, microbes, and the environment, experiments performed under controlled conditions, at a particular stage of plant development, or in the absence of a native microbial community, fail to capture the spatial and temporal heterogeneity of the field. One way to bridge the gap, at least in part, is to screen for plant growth promotion at the community level—either with wild soil inoculum or a pre-defined syncom—resulting in levels of ecological complexity better approximating field conditions. Additionally, communities identified as plant-beneficial can include members with synergistic interactions and/or functional redundancy to support both initial colonization and persistence in the soil (Zhuang et al. 2021; Kaur et al. 2022; Liu et al. 2022). Because of these synergies and functional redundancy, syncoms may even have greater resilience to functional shifts across environmental heterogeneity compared to single-isolate inoculations alone (Bradáčová et al. 2019).

However, syncoms are often designed around *a priori* knowledge of individual isolates rather than taking a community-oriented approach (Vorholt et al. 2017). Isolate-first approaches usually aim to saturate a syncom with individuals known to perform a particular function, and might additionally screen isolates for stable pairwise interactions (Herrera Paredes et al. 2018; Faust and Raes 2012; Friedman, Higgins, and Gore 2017). While these approaches have resulted in syncoms with demonstrated plant-beneficial effects (e.g. Herrera Paredes et al. 2018), they quickly become prohibitively time and labor-intensive as the number of isolates to be screened increases. Nearing a community-level approach, others have attempted to traverse the isolate sample space by recapitulating simplified versions of naturally assembled communities (B. Niu et al. 2017), or otherwise modeling species interactions based on known patterns of co-occurrence or syntrophy (H. Wang et al. 2017; Jones and Carlson 2019; McCarty and Ledesma-Amaro 2019).

We propose that host-mediated selection has been an underutilized framework for microbiome engineering, one that inherently accounts for ecological interactions within a microbiome without requiring *a priori* knowledge about them. In brief, host-mediated selection uses host phenotype as a reporter to artificially select microbiomes associated with desirable host phenotypes (U. G. Mueller and Sachs 2015; Ulrich G. Mueller and Linksvayer 2022). By targeting the emergent property of a microbiome (i.e. its impact on host phenotype), selection occurs at both the individual microbe and microbial community levels to maintain or exclude

specific taxa and interactions (Whitham et al. 2020). In other words, host-mediated selection not only identifies taxa with direct benefit to host phenotype, but also identifies taxa that indirectly benefit their plant hosts via their interactions with other microbiome members.

Here, we describe a long-term experiment where we applied host-mediated selection to derive simplified root microbiomes that enhance rice drought tolerance. Drought severely reduces rice production and threatens the food security of billions of people around the globe (Panda, Mishra, and Behera 2021; Pandey and Shukla 2015). On the other hand, cultivation in flooded paddies emits significant amounts of methane and nitrous oxide, leading rice to account for nearly half of greenhouse gas emissions from croplands (Qian et al. 2023). Consequently, discovering new ways to cultivate rice with less water can be of benefit to both people and the environment. In addition to identifying bacterial communities and individual taxa with the potential to enhance rice drought tolerance, we also contribute to the nascent body of microbiome engineering literature by comparing outcomes of host-mediated selection applied to diverse sources of inocula.

Results

To start, we established four soil treatments, three of which were inoculated with diverse field-collected soil microbiota; the fourth treatment received no initial inoculation and was left to acquire microbes from the environment alone. Each soil treatment further consisted of multiple selection and control lines (**Figure 1**). Each Selection Line (SL) included 15 plants per generation from which 3 were selected and their microbiomes harvested to inoculate a subsequent generation of 15 plants. Importantly, selection lines were independent of one another, and “generation” refers to a 40 day selection cycle rather than a seed to seed cycle. No drought treatment was applied in the first generation, with the intent to simply enrich microbiota associated with healthy rice roots to start. Accordingly, we refer to this selection cycle as the Enrichment Generation (EG) and subsequent selection cycles as Selection Generations (SG), during which rice plants were challenged with a 10 day drought treatment after 30 days of well-watered growth. Each soil treatment also included two control lines, one Sterile-Inoculated (SI) and the other Live-Inoculated (LI). In contrast to selection lines, each of the two control lines included 30 plants per generation, and microbiomes were not selected for propagation forward into future generations. Instead, both control lines were intended to provide meaningful contrasts to selection lines: SI underwent the same drought treatment as selection lines, but received sterilized versions of selection line inocula; LI were never droughted but received unsterilized inocula from selection lines. Simply put, SI plants were meant to serve as a static control for rice drought performance across generations; LI plants were meant to help identify microbes enriched by drought specifically, and to determine whether microbiomes optimized for drought were deleterious to the performance of unstressed plants (See **Figure 1** and Methods for greater detail on experimental design, rice phenotyping methods, inoculum preparation, and selection criteria). Comprehensive reviews of host-mediated selection experimental design and terminology can also be found in Mueller and Sachs 2015 and Mueller and Linksvayer 2022 (U. G. Mueller and Sachs 2015; Ulrich G. Mueller and Linksvayer 2022).

Source inocula bacterial diversity

Without specific *a priori* expectations of which microbial taxa or functions would be required to improve drought tolerance in rice, we first screened a panel of nine field soils from distinct ecoregions and land-use histories across California for rice growth phenotypes. Each soil was characterized by unique physico-chemistry and bacterial diversity, even at broad taxonomic levels (**Figure 2, Supplemental Figure 1, Supplemental Table 1**). And, after inoculating rice plants with each of the soils, we observed differences in rice growth phenotypes between soil inoculation groups (**Supplemental Figure 1D-F**). Of the field soils whose microbes better supported rice growth, we chose three to use as source inocula for host mediated selection: Rice Field, from a fallow rice field; Desert, from the Mojave Desert; and Serpentine Seep, from a serpentine soil that experiences consistent groundwater seep. In addition to their relatively beneficial impact on rice plants within our pilot experiment, we chose these soils for their negligible overlap in taxonomic composition, which would provide host-mediated selection with three distinct starting points. Further, we reasoned that each soil community might have its own set of advantages: Rice Field microbes might be more likely to form associations with rice roots and tolerate flooded conditions; Desert taxa might be better adapted to drought; and the diversity of Serpentine Seep taxa, in terms of both richness and evenness, might provide more functional diversity for host-mediated selection to act upon. Just prior to host-mediated selection, we collected fresh field samples of Rice Field, Desert, and Serpentine Seep soils. For good measure, we characterized the bacterial diversity of these new collections, the results of which were consistent with what we had previously observed (**Figure 2C, Supplemental Figure 1**). The fourth soil treatment included in host-mediated selection, Calcined Clay, received no field soil inoculum; as the name of this treatment suggests, the first generation of these plants was sown directly into sterilized calcined clay substrate.

Rice phenotypes improve across selection generations

To assess drought tolerance in our system, we created a non-destructive, image-based protocol to measure the Normalized Difference Vegetation Index (NDVI) of individual plants during drought. Briefly, NDVI is a metric that quantifies plant stress by measuring the intensities of red and infrared light reflected by leaf surfaces and is most commonly used in remote sensing to determine plant health (Rouse et al. 1974; Huang et al. 2021). Prior to host-mediated selection we performed an additional pilot experiment confirming that measured values of NDVI drop as drought intensity increases (**Supplemental Figure 2D**); these values also had strong correlation with plant shoot percent water content (R=0.98, p<2.2e-16; **Supplemental Figure 2E**). Additional information about our protocol can be found in the Methods as well as in **Supplemental Figure 2**.

In the context of host-mediated selection, we observed consistent, significant increases in both NDVI across selection generations for Rice Field, Desert, and Calcined Clay soil treatments, but not for Serpentine Seep (**Figure 3**). Specifically, the area under the curve of NDVI values throughout drought (AUC NDVI) significantly increased in all selection lines (SLs) belonging to Rice Field (6/6), Desert (6/6), and Calcined Clay (3/3), but in just two SLs belonging to Serpentine Seep (2/6) (**Figure 3B, Supplemental Figure 3A**). In further contrast to the improved performance of other soil treatments, two Serpentine Seep SLs significantly decreased AUC NDVI across selection generations (**Supplemental Figure 3A**).

Notably, the improvements in AUC NDVI of non-Serpentine Seep soil treatments did not come at the expense of plant biomass (**Figure 3C**). Rather, shoot biomass generally increased over time, with results similar to AUC NDVI: all Rice Field (6/6) and Calcined Clay (3/3) SLs, and most Desert SLs (5/6), significantly increased shoot biomass across selection generations. Two Serpentine Seep SLs showed significant change over time, with one (1/6) increasing and the other (1/6) decreasing in biomass (**Supplemental Figure 3B**). Sterile-inoculated (SI) control lines of all soil treatments, Serpentine Seep included, also saw significant increases in both AUC NDVI and biomass phenotypes over time (**Figure 3, Supplemental Figure 3**). Though each SI plant received sterilized inoculum and was maintained as a spatially discrete unit (**Supplemental Figure 4**), they were not axenic; consequently, SI plants were colonized by environmental microbiota throughout each 40-day generation. Overall, given that environmental conditions and rice genotypes were held constant across selection generations, these data suggest that changes in microbiome composition and function were driving improvements in rice drought phenotypes, even in SI plants.

Microbiome diversity and composition over time

To assess the impact of host-mediated selection on bacterial community composition and diversity across selection generations, we performed 16S rRNA sequencing on all root samples from Rice Field (n = 1019) as well as a subset of those from Desert (n = 58) , Serpentine Seep (n = 58), and Calcined Clay (n = 42) soil treatments. At the start, high microbial diversity was observed across all soils, Serpentine Seep exceptionally so, with higher levels of species richness (2507 observed ASVs) and evenness (Shannon Index = 7.1) compared to Rice Field (1390 observed ASVs; Shannon Index = 6.3) and Desert soils (869 observed ASVs, Shannon Index = 6.1) (**Figure 4A-B**). Within several selection generations, however, bacterial communities of all soil treatments had been reduced to just ~200 ASVs. While diversity decreased steadily over time in Rice Field microbiomes, both Desert and Serpentine Seep lost most of their input diversity in the enrichment generation (EG) alone (**Figure 4A-B**). Considering that only roots from EG plants were harvested to inoculate plants in SG1, the large reduction in diversity during EG is consistent with the observation that microbial diversity generally declines along transects spanning from bulk soil to root endophytic spaces (Kuzyakov and Razavi 2019). Additionally, Rice Field better maintained diversity in this first generation, supporting our initial hypothesis that this soil would be more likely to include taxa that associate with rice roots. In contrast to the field soil treatments, Calcined Clay SL microbiomes saw modest increases in diversity between EG (78 observed ASVs; Shannon Index = 2.9) and SG4 (138 observed ASVs; Shannon Index = 3.6), consistent with the fact that this treatment did not receive a field soil inoculum in EG, but was allowed to recruit microbiota from the growth chamber environment (**Figure 4A-B**). Similarly, sterile-inoculated plants successfully recruited microbes from the environment each generation, though the resulting communities were consistently less diverse compared to their selection line counterparts (**Figure 4A-B**).

Next, we assessed the impact of host-mediated selection on bacterial community beta diversity using Bray-Curtis dissimilarity, which is particularly useful for showing changes in community composition along a gradient or through time (Anderson et al. 2011). Though soil treatments maintained distinctive microbiome identities throughout the experiment, their community compositions became increasingly similar across selection generations (**Figure 4C,**

Supplemental Figure 5A,C). Within each soil treatment, SL and SI bacterial communities formed distinct clusters, but changes in their composition also followed similar trajectories over time (**Figure 4D-G**). Because Bray-Curtis is not a true distance metric and required rarefaction to normalize read counts between samples, we additionally quantified Aitchison distance which does not rely on rarefaction and is explicitly intended for compositional data (Martino et al. 2019). Both metrics were generally in agreement and confirmed that microbiomes of different soil treatments increased in similarity over time (**Supplemental Figure 5A,C**). Within field soil treatments—Rice Field, Desert, and Serpentine Seep—both metrics also show SL microbiomes becoming more similar to their sterile-inoculated counterparts over time, with the exception of Desert which is static over time by Aitchison distance (**Supplemental Figure 5B,D**). Differences between Calcined Clay SL and SI, on the other hand, were static when measured by Bray-Curtis, and increased over time when measured by Aitchison distance. To confirm that the overall increase in similarity between soil treatments was not solely driven by shared sparsity, we simply counted the number of ASVs shared between SL plants of each soil treatment: in the enrichment generation, just 0.4% (28/7106) of observed ASVs were shared by three or more soil treatments, increasing to 4.3% (107/2471) by SG4 (**Supplemental Figure 6A**). Moreover, shared ASVs tended to be more abundant, with a subset of just 20 shared ASVs eventually accounting for up to 60% of microbiome composition in SG4 (**Supplemental Figure 6B**).

Dispersal and growth rate influence bacterial fitness

Given the trend towards more uniform community composition both within and between soil treatments over time, we sought to better understand whether shared ASVs represented a common set of taxa recruited from the growth chamber environment or if taxa dispersed between soil treatments. To do so, we assigned ASVs as originally belonging to one or multiple soil treatments based on which original field soils and EG inocula they were observed in. Mapping these designations onto the bacterial community data, it became clear that shared ASVs were the result of dispersal events between soil treatments as well as recruited from the environment (**Figure 5**). Environmental bacteria quickly rose to high abundance in all soil treatments— as much as 50% of relative abundance by the end of SG1—and remained a significant fraction of the community throughout subsequent selection generations. Despite the colonization of non-native bacteria, the native diversity of Rice Field and Serpentine Seep SL microbiomes remained the dominant fraction, whereas the native diversity of Desert SL microbiomes steadily declined. Calcined Clay microbiomes, initially uninoculated, were primarily composed of environmental taxa with the remaining fraction evenly represented by treatments inoculated with field soils. Interestingly, microbiomes of SI plants were biased towards the diversity of their respective soil treatments, though the fraction of native diversity in these communities was consistently less compared to their SL counterparts (**Figure 5**); this bias was likely the result of dispersal limitation, priority effects, or both, given that plants were regularly shuffled within—but not between—soil treatments during each generation. Overall dispersal proved to be a fitness advantage in the context of host-mediated selection by increasing a taxon's likelihood of being observed in a selected microbiome and allowing re-inoculation in lines where the taxon was lost due to either host-mediated selection or stochastic drift.

Because dispersing taxa enjoyed a fitness advantage within our selection scheme, we wondered if other general bacterial traits, like growth rate, similarly influenced selection. To test

255 whether microbiomes became biased towards fast-growing taxa over time, we estimated the
256 mean doubling time of ASVs observed in SL and SI plants at each generation. Specifically, we
257 aligned our 16S rRNA amplicon sequences to the Estimated Growth rates from gRodon Online
258 (EGGO) database, which includes predicted growth rates for more than 200,000 bacteria and
259 archaea, and assigned a doubling time to each ASV in our Rice Field dataset (Weissman, Hou,
260 and Fuhrman 2021). While we found sterile-inoculated microbiomes to be biased towards fast-
261 growing taxa in all generations, selection line microbiomes became biased toward fast-growing
262 taxa over time (**Figure 6**). Though this analysis offers a coarse view of average growth rates
263 within communities, the bias towards fast-growing taxa in SI, compared to SL microbiomes, is
264 consistent with the fact that rapid colonization of unoccupied space—i.e. SI roots at the start of
265 each generation—often results in a fitness advantage (López et al. 2023; Debray et al. 2022).
266
267 ***Selection strength diminishes over time***
268 Having observed the effects of individual selective forces on community composition,
269 e.g. strong environmental and host-mediated filtering (**Figure 4**) as well as abundance patterns
270 influenced by dispersal and growth rate (**Figures 5-6**), we sought to better their overall
271 contribution to microbiome assembly through time. To do so, we determined the extent to which
272 Rice Field selection line microbiomes deviated from a neutral community model in each
273 generation (**Supplemental Figure 7**). A neutral community model assumes that microbiome
274 assembly is the result of stochastic dispersal and drift, and that all individuals have equal
275 fitness; accordingly, deviations from neutrality indicate that community assembly was influenced
276 by non-neutral processes, e.g. active dispersal or differential fitness (Sloan et al. 2006). For
277 each generation, we used abundance data from the previous generation as our source
278 community to parameterize migration and replacement rates and confirmed that this step
279 improved model fit compared to random subsampling as in Burns et al. 2016 (Burns et al.
280 2016). Assessing the overall fit of the neutral models via generalized R^2, we found that model fit
281 improved across selection generations (SG1: R^2=0.109; SG6: R^2=0.558; **Supplemental Figure**
282 **7**). This result suggests that host-mediated selection had a strong influence on microbiome
283 assembly in early selection generations and increasingly stabilized communities. However,
284 because neutral model fit was still poor in SG6, non-neutral processes were still actively
285 determining microbiome assembly in late selection generations.
286
287 ***Identification of phenotype-associated taxa***
288 Using Rice Field microbiomes, we followed several lines of inquiry that identified a small
289 subset of taxa most likely responsible for improvements in host phenotypes. We used Rice Field
290 data for these analyses because, for logistical reasons, we focused our resources on this soil
291 treatment by performing an additional two selection generations and sequencing all root-
292 associated samples (*n*=1019). Our first two analyses were straightforward, simply asking 1)
293 which ASVs were most abundant in the final selection generation and 2) which ASVs were
294 differentially abundant in droughted versus watered microbiomes. To answer the first question,
295 we ranked ASVs by their mean relative abundance in SG6 and found that one in particular, a
296 species of *Ideonella*, was the dominant taxon across all selection lines (mean relative
297 abundance = 33%) as well as sterile- (25%) and live-inoculated (21%) lines (**Supplemental**
298 **Figure 8**). Combining this *Ideonella* with the next top ten most abundant ASVs accounted for

299 more than half of SL microbiome relative abundance in SG6 (60%), and nearly half in SI (45%)
300 and LI (47%) microbiomes (**Supplemental Figure 8**). In total, these top 11 ASVs were
301 represented by five Proteobacteria (from the genera *Ideonella*, *Azospirillum*, *Asticcacaulis*, and
302 two within the family *Rhizobiaceae*), two Actinobacteriota (representing *Streptomyces* and
303 *Nocardioides*), and one each from the phyla Bacteroidota (*Flavisolibacter*), Fibrobacterota
304 (*Fibrobacteraceae*), Myxococcota (*Kofleraceae,* likely *Haliangium*), and Verrucomicrobiota
305 (possible *Chthoniobacteraceae* or *Terrimicrobiaceae*).
306 To answer our second question—which ASVs were enriched in either drought or
307 watered conditions—we measured the differences and effect size of median CLR-transformed
308 abundances of ASVs between selection line (droughted) and live-inoculated (watered)
309 conditions. We then stringently filtered data to only keep ASVs where enrichment in one
310 condition or another was significant after FDR correction, with effect sizes greater than +/- 0.5,
311 and having met these criteria in at least three selection generations. Those remaining included
312 30 ASVs identified as drought-enriched, as well as 30 ASVs identified as water-enriched
313 (**Supplemental Figure 9**). Of note, Actinobacteriota made up an outsized proportion of drought
314 indicators given the total diversity of Actinobacteriota ASVs observed ($p<0.05$, one-sided
315 Fisher's exact test, **Supplemental Figure 9**); by contrast Proteobacteria were the most
316 represented phylum among both drought and water indicators, though this group was also the
317 most diverse throughout the experiment (**Supplemental Figure 9, Figure 7A**). Overall, water
318 indicators were more diverse at the phylum level (**Supplemental Figure 9**).
319 Next, we sought to specifically identify ASVs likely driving growth promotion and
320 improved NDVI scores (**Figure 7**). By mapping which ASVs showed strong positive or negative
321 correlations with plant biomass and AUC NDVI onto a phylogenetic tree, it became clear that
322 though these taxa spanned most of the tree—including many major phyla—there were also
323 several notable clusters representative of genus-level clades with consistent responses
324 associated with host phenotype (**Figure 7A**). Further, many of the most abundant taxa in the
325 final selection generation—outlined above—also strongly correlated with enhanced rice drought
326 tolerance. Notably, multiple *Bacillus* ASVs also exhibited strong association with improved rice
327 drought performance, despite their lower relative abundances in SG6 (ranging from 0.50-0.67%,
328 **Figure 7A**). ASVs identified as belonging to subphyla I and III of the Chloroflexi stood out as
329 strongly negatively correlated with both NDVI and biomass phenotypes (**Figure 7A**).
330 We then used the correlation data to recombine ASVs into balances to find
331 subcompositions of ASVs predictive of phenotypes (**Figure 7C**). In brief, balances acknowledge
332 the compositional structure of microbiome data and that information is therefore carried in the
333 ratios between components (e.g. ASVs); balances, then, are a ratio of the geometric means of
334 two groups of taxa which can be used to predict a continuous phenotype (Rivera-Pinto et al.
335 2018; Morton et al. 2017). We constructed balances separately for AUC NDVI and shoot
336 biomass phenotypes, where the numerator and denominator groups included taxa positively
337 and negatively associated with phenotype, respectively. In total, the AUC NDVI balance
338 included 32 ASVs (numerator = 17, denominator = 25) and the shoot biomass balance included
339 53 ASVs (numerator = 36, denominator = 17). Both balances showed exceptionally strong
340 correlations to phenotypes, with Pearson correlation coefficients as high as 0.87 and 0.62 for
341 AUC NDVI and shoot biomass, respectively (**Figure 7C**). Though balances were constructed

342 from selection line data only, they performed nearly as well applied to sterile-inoculated sample
343 data (**Figure 7C**; AUC NDVI: R=0.65; shoot biomass: R=0.41)
344
345 ***Functional enrichments among phenotype-associated taxa***
346 Finally, we sought to identify gene functions enriched among our selected taxa in order
347 to better understand the forces potentially influencing their selection during the experiment. To
348 do so, we conducted shotgun metagenomics on a subset of samples from Rice Field selection
349 line plants across all 7 generations (n=37); from this data, we resolved 272 high quality
350 metagenome-assembled genomes (MAGs). To allow for correlations between functional
351 capacity in our metagenomic dataset and the much greater temporal and phenotypic resolution
352 afforded us by our 16S dataset, we assigned individual MAGs to ASVs from the 16S dataset
353 using a combination of taxonomic and abundance data. Next, we identified Clusters Of
354 Orthologous Genes (COG) high-level functional categories with significant enrichments in gene
355 counts among phenotype-associated taxa; specifically, we ran two parallel analyses using the
356 taxa included in the numerators of each of the balances (AUC NDVI and shoot biomass)
357 described above (**Figure 8**). As background for each analysis, we used all ASV-matched MAGs
358 (n=165). After applying FDR corrections to p-values and filtering for significance ($p<0.05$) we
359 found that the groups of MAGs associated with both balances were significantly enriched for
360 genes within the functional categories *Carbohydrate transport and metabolism* and
361 *Transcription* compared to non-selected MAGs. Notably, there were also differences between
362 enrichment profiles for the AUC NDVI and shoot biomass MAG sets; specifically, MAGs from
363 the AUC NDVI-related balance showed significant enrichment of genes related to *Cell motility*,
364 *Inorganic ion transport and metabolism*, and *Intracellular trafficking, secretion, and vesicular*
365 *transport*, while the biomass-related balance MAGs showed significant enrichment of *Lipid*
366 *transport and metabolism* and *Secondary metabolite biosynthesis, transport and catabolism*.
367 Within these significantly enriched high-level COG functional categories associated with
368 each group, we repeated the same processes above to identify individual COGs with enriched
369 gene counts. Taxa associated with improved AUC NDVI showed specific enrichment of genes
370 related to iron transport (COG1629), flagellar structure (COG1344), as well as a diverse array of
371 COGs related to sugar transport and metabolism (**Supplemental Figure 10**). Interestingly, both
372 groups showed significant enrichment for COGs associated with glycerol-3-phosphate transport
373 (COG1653, COG0395, **Supplemental Figure 11**), a bacterial function identified in recent
374 studies as correlated with drought tolerance in rhizosphere communities (L. Xu et al. 2018).
375 Together, these results suggest that bacteria selected in our experiment are enriched for
376 specific microbial functions associated with transport of a range of metabolic products and
377 nutrients compared to other non-selected taxa in our system.

378 Discussion

379 Here, we present a multi-generation experiment in which we applied host-mediated
380 selection to diverse sources of inocula to derive simplified soil communities that promote growth
381 and drought tolerance in rice. One of our primary motivations for this experiment was to
382 determine the degree to which inoculum source matters, or if any microbial community can
383 serve as a suitable substrate for host-mediated selection. Though microbial communities adapt

384 to their local environments and are therefore biased towards specific taxa and functions
385 (Kraemer and Boynton 2017; Bokulich et al. 2014; Fierer and Jackson 2006; Bååth 1996), we
386 reasoned that any sufficiently diverse community would include members capable of inducing a
387 targeted host phenotype (Delgado-Baquerizo et al. 2016). These members could then be
388 maintained or enriched via host-mediated selection if selection were sufficiently strong relative
389 to stochastic effects or other factors influencing microbial fitness (Belotte et al. 2003; Kraemer
390 and Kassen 2015). Here, however, soil treatments differed in their response to host-mediated
391 selection, where Rice Field and Desert successfully improved rice phenotypes over time but
392 Serpentine Seep did not (**Figure 3**). Interestingly, selection maintained native diversity in Rice
393 Field microbiomes, but preferentially enriched bacteria acquired via immigration in Desert ones
394 (**Figure 5**). We suspect that Rice Field better maintained diversity because its source inoculum
395 likely included more taxa that are better adapted to flooded conditions and capable of colonizing
396 rice roots. Given that plant hosts both actively and passively influence microbial colonization
397 (Zhang et al. 2023; B. Wang and Sugiyama 2020; Johnson et al. 2010), the latter may have
398 been of particular importance because roots—but not soil—were harvested from EG plants to
399 inoculate SG1. However, even Calcined Clay, which relied solely on immigration for microbiome
400 assembly in EG, successfully responded to host-mediated selection. Taken together, these
401 results suggest that source inoculum provenance strongly influenced the trajectory of host-
402 mediated selection, but was just one of many factors determining its outcome.
403 Dispersal also played an evident role in microbiome assembly in all soil treatments.
404 Despite negligible overlap in shared species at the start of the experiment, all soil treatments
405 generally converged toward a common set of taxa rather than solving the phenotypic "problem"
406 with unique solutions (**Figure 4C, Supplemental Figures 5-6**). Consistent with this observation,
407 others have shown that even low rates of dispersal can homogenize a metacommunity
408 (Fodelianakis et al. 2019). In particular, when factors determining bacterial fitness—i.e.
409 environmental conditions, plant host genotype, and artificial selection criteria—are consistent
410 throughout the metacommunity, dispersal has an even greater homogenizing effect (Evans,
411 Martiny, and Allison 2017; Bell 2010; Kraemer and Kassen 2015). Using the Desert soil
412 treatment as an example, immigrating taxa appeared to enjoy a fitness advantage over the
413 native diversity of the field soil within the context of host-mediated selection; as a result, these
414 taxa were selected and further enriched over time, increasing the compositional similarity
415 between Desert and other soil treatment microbiomes.
416 As microbiome compositions changed across selection generations, we observed clear
417 patterns of maintenance and enrichment of taxa positively correlated with the rice phenotypes
418 under artificial selection. Many of these taxa are members of genera that include well-known
419 plant growth promoting rhizobacteria (PGPR), including *Azospirillum* (Proteobacteria) and
420 *Bacillus* (Firmicutes), both of which have previously been shown to improve rice growth and
421 drought tolerance (Fukami, Cerezini, and Hungria 2018; Ruíz-Sánchez et al. 2011; Sansinenea
422 2019; Karmakar et al. 2021). Actinobacteriota, particularly *Streptomyces* and *Nocardioides*,
423 increased in relative abundance over time as well, but were also consistently enriched in
424 droughted (SL) compared to watered (LI) microbiomes (**Supplemental Figure 9**). Many other
425 studies have similarly reported the enrichment of root-associated Actinobacteriota during
426 drought (Naylor et al. 2017; L. Xu and Coleman-Derr 2019; Santos-Medellín et al. 2017;
427 Fitzpatrick et al. 2018) and have also demonstrated *Streptomyces* capable of inducing drought

428 tolerance in grasses, including rice, through osmolytic balancing, reduction of ROS, and auxin
429 production (S. Niu et al. 2022; Selim et al. 2019; Yandigeri et al. 2012).
430 We also identified taxa that strongly correlated with improved rice drought tolerance, but
431 for which little is known about their potential for plant growth promotion. For example, we
432 observed the enrichment of two Proteobacterial genera, *Devosia* and *Ideonella*, whose
433 abundances strongly correlated with enhanced NDVI and biomass phenotypes. While there
434 appeared to be multiple beneficial strains of *Devosia* enriched through host-mediated selection,
435 a single *Ideonella* ASV reached exceptionally high relative abundances in SG6 Rice Field
436 microbiomes (**Supplemental Figure 8**). Isolates described for both genera appear to have
437 several characteristics in common, including production of siderophores and auxin, as well as
438 the ability to fix atmospheric nitrogen (Rivas et al. 2003; Chhetri, Kim, Kang, Kim, et al. 2022;
439 Chhetri, Kim, Kang, So, et al. 2022). Though literature describing interactions of *Devosia* and
440 *Ideonella* with plants is sparse, *Devosia* has been shown capable of nodulating an aquatic
441 legume (Rivas et al. 2003), and members of *Ideonella* can promote the growth of eucalyptus
442 seedlings (De Sousa Fabiano Gama et al. 2022). Overall, our ability to identify PGPR—ranging
443 from well-known to poorly characterized—suggests that host-mediated selection is not only
444 useful for microbiome engineering, but can also be used to identify novel species of plant-
445 beneficial microbes.
446 Additionally, we identified balances, or subcompositions of taxa, that significantly
447 improved predictions of rice phenotypes compared to the abundance data of individual taxa
448 alone (**Figure 7**). Interestingly, the balances—constructed separately for AUC NDVI and shoot
449 biomass phenotypes—showed little overlap with one another, despite the fact that many of the
450 ASVs included in the balances were strongly correlated with both phenotypes (**Figure 7A**). This
451 suggests that discrete subcompositions of the microbiome were important for determining NDVI
452 and biomass, separately. While balance numerator groups represent a short list of potential
453 PGPR and candidates for syncom construction, denominator groups represent taxa more likely
454 to hinder plant phenotypes with increased abundance. Though balances were constructed from
455 Rice Field selection line data, they may help to explain the failure of Serpentine Seep to
456 respond to host-mediated selection: Chloroflexi were overrepresented in the denominator group
457 for AUC NDVI and was also the phylum designation of the most abundant ASV in final
458 generation Serpentine Seep plants. Balances also corroborate that phenotypic improvements
459 observed across selection generations in sterile-inoculated plants corresponded to similar
460 changes in microbiome composition experienced by their selection line counterparts.
461 By comparing metagenome-assembled genomes (MAGs) associated with our selected
462 taxa (balance numerators) to all other MAGs in the dataset, we identified specific functions
463 enriched in selected taxa that could help to explain their positive correlation with phenotypes.
464 Supporting the hypothesis that balance groups had discrete effects on either AUC NDVI or
465 shoot biomass phenotypes, few enriched functions were shared between the two groups. This
466 result is perhaps not unexpected given that the two balances were composed of different sets of
467 taxa, but it does enable a closer look at which functions were important for each phenotype
468 individually. For example, genes related to both iron transport (COG1629) and carbonic
469 anhydrase (COG3338) were significantly enriched by the numerator group for AUC NDVI but
470 not shoot biomass (**Supplemental Figure 10**). Previous work has specifically demonstrated iron
471 transport and metabolism as important functions for Actinobacterial-mediated drought tolerance

472 in sorghum (L. Xu et al. 2021) and carbonic anhydrase as a potential mechanism for *Bacillus*-
473 mediated drought tolerance in wheat (Aslam et al. 2018). By comparison, genes associated with
474 both lipid and secondary metabolite transport showed strong enrichment within MAGs belonging
475 to the numerator group for biomass. Lipids have been identified as a key avenue of
476 communication between hosts and microbes during plant microbe interactions, including
477 beneficial symbioses (Siebers et al. 2016). Additionally, on the list of significantly enriched
478 secondary metabolite COGs are cytochrome P450s, which are capable of producing a wide
479 array of many small molecules, including phytohormones and other compounds used by
480 microbial partners to manipulate plant fitness (Orozco-Mosqueda, Santoyo, and Glick 2023).
481 Interestingly, both AUC NDVI and biomass balances showed strong enrichment for
482 COGs associated with G3P transport and metabolism (COG1653, COG0395). Prior work in
483 another plant system (*Sorghum bicolor*) has found a correlation between G3P transport in
484 Actinobacteriota and their tolerance to drought stress within the rhizosphere environment (L. Xu
485 et al. 2018); it was hypothesized that this correlation may be due to significant increases in G3P
486 production observed in plants exposed to drought stress (L. Xu and Coleman-Derr 2019).
487 Interestingly, our data suggest that transport of G3P may also be an important function in
488 drought-related contexts outside the Actinobacteriota, as G3P transport-related genes were
489 present and enriched across multiple phyla represented in our balance numerator taxa,
490 including Actinobacteriota as well as Armatimonadota, Bacteroidota, Firmicutes, Myxococcota,
491 Proteobacteria, and Verrucomicrobiota. Furthermore, the fact that our MAGs were selected
492 based on their associations with hosts exhibiting enhanced drought tolerance, rather than on
493 their own ability to survive drought, suggests that G3P metabolism and transport may play a
494 specific role in meditating mutualistic interactions between plants and microbes under water
495 stress.
496 Overall, this study demonstrates that host-mediated selection efficiently operates at the
497 community level to reduce microbiome complexity and enrich functions of interest. In the context
498 of the nascent body of host-mediated selection literature, it also provides further insight into
499 numerous aspects of experimental design that can present challenges to successful community
500 selection. For instance, the use of appropriate control lines is prudent, but difficult to implement.
501 Specifically, in our study, dispersal complicated our efforts to utilize the sterile-inoculated (SI)
502 lines as meaningful controls. Rather than statically recruiting the same environmental microbes,
503 SI plants recruited microbes from an increasingly optimized metacommunity each generation.
504 Consequently, sterile-inoculated plants saw phenotypic improvements similar to their selection
505 line counterparts. The shared trajectory of selection and intended control lines appears to be a
506 consistent phenomenon—to varying degrees—in other host-mediated selection studies (Panke-
507 Buisse et al. 2015; King et al. 2022; Garcia et al. 2022; Kalachova et al. 2022; Rodríguez et al.
508 2023). “Add-back” controls—where hosts are inoculated from a stock source of the original
509 inoculum at the start of each generation—were subject to the same phenomenon, though to a
510 lesser extent compared to sterile-inoculated or “random-selection” controls (King et al. 2022;
511 Garcia et al. 2022). The use of fully gnotobiotic plants could eliminate this issue, but would be
512 both challenging and expensive to implement for most plant species.
513 Additionally the length of experimental generations influences whether slow-growing
514 microbial species are maintained in selected communities and determines the likelihood of
515 community turnover within a generation (Wright, Gibson, and Christie-Oleza 2019). Short

516 generation times correspond to high dilution rates (i.e. how frequently microbiomes are
517 selected) and can result in dilution to extinction (Adamberg and Adamberg 2018; Díaz-García et
518 al. 2021; Xie and Shou 2021). Despite our efforts to make generations as long as possible
519 (harvesting plants after 40 days of vegetative growth, before source-sink relationships begin to
520 change with the onset of heading), we still observed selection biased towards fast-growing taxa
521 (**Figure 6**). This may be due in part to the fact that rapid growth can also provide fitness
522 advantages, particularly by influencing priority effects in early stages of microbiome assembly
523 (López et al. 2023; Whitman et al. 2018; Debray et al. 2022). While longer generations may help
524 to maintain slow-growing taxa, they also increase the likelihood of community turnover, which is
525 problematic if taxa driving the phenotype of interest are displaced before they can be transferred
526 to the next generation (Wright, Gibson, and Christie-Oleza 2019). In short, we encourage others
527 attempting host-mediated selection to consider the ways in which experimental design might
528 weaken the strength of artificial selection or otherwise limit the number of potential routes
529 microbiome selection can take.

530 # Conclusion

531 Microbiomes have the potential to increase agricultural sustainability and productivity,
532 yet engineering beneficial plant microbiomes remains largely intractable. One of the primary
533 challenges is accurately predicting which microbes will cooperatively improve host phenotype
534 under heterogeneous field conditions. Screening large isolate collections for specific plant
535 growth promoting functions can be a costly and time-consuming process and ultimately fails to
536 account for interactions between microbes, the plant host, and the environment. An approach
537 like host-mediated selection, however, significantly simplifies the process of microbiome
538 engineering by allowing eco-evolutionary processes to optimize microbiome composition at the
539 community level. In other words, host-mediated selection inherently accounts for microbe-
540 microbe interactions (including higher order interactions) while identifying individuals and
541 consortia that are beneficial to plant phenotype. Moreover, selected communities not only
542 provide a blueprint for syncom design but are also a source from which phenotype-promoting
543 taxa can be more readily isolated. From our work, we show that although experimental design
544 must be carefully considered to ensure the greatest chances of success, host-mediated
545 selection holds great promise for identifying and mining plant beneficial taxa from complex soil
546 environments.

547 # Methods

548 ***Rice growth conditions***

549 We used a near isogenic rice japonica cultivar known as “Super Dwarf” (*Oryza sativa* L.),
550 which is a gibberellic acid mutant that grows vigorously, but only reaches heights of around
551 20cm at maturity (Frantz and Bugbee 2002). We initially bulked seeds through selfing until we
552 acquired enough material for the entire experiment and stored these at 4˚C. Prior to each
553 generation, seeds were surface sterilized then germinated in sealed 50 ml falcon tubes filled
554 with autoclaved milliQ water at 28˚C for five days before being transplanted into inoculated

555 substrate. To minimize cross contamination between replicates, each plant was grown in an
556 individual, autoclave-sterilized “conetainer” (Greenhouse Megastore, catalog No. SC10R) and
557 given a separate water reservoir (Restaurant Equipment Solutions, catalog No. LIBB-551HT)
558 (**Supplemental Figure 4A**). We built custom racks to hold five plants each to allow rotation of
559 plants within a soil treatment to normalize environmental and ballast exposure over the course
560 of the generation (**Supplemental Figure 4B**).
561 The entirety of this experiment was performed in a walk-in growth chamber
562 (**Supplemental Figure 4B**); conditions were set to 16-hour days, during which daytime
563 temperature and humidity were held at 28˚C and 80%, respectively, and relaxed to 24˚C and
564 75% humidity at night. Once transplanted, rice were grown for a total of 40 days. We fertilized
565 plants with 10mL 1X Murashige and Skoog medium at the time of planting, and again on days 7
566 and 14; on day 21 we applied a final fertilization of 10mL 0.5X 20-20-20 NPK. We previously
567 observed that this level of fertilization was growth-limiting but not stress-inducing. Plants were
568 consistently well-watered with milliQ water throughout the enrichment generation; in subsequent
569 selection generations, a drought treatment was initiated after 30 days of well-watered growth.
570 On day 31, we emptied water reservoirs and allowed the formerly flooded substrate to drain
571 before refilling the reservoir to 25% full capacity; we repeated this emptying and refilling again
572 the following day. On day 33 reservoirs were emptied without refilling and water was withheld
573 for the remainder of the generation.
574
575 ***NDVI measurements***
576 To non-destructively phenotype plants in high throughput, we built custom hardware and
577 computational scripts to measure Normalized Difference Vegetation Index (NDVI) of individual
578 plants longitudinally. Originally developed for remote sensing applications, NDVI is commonly
579 used to track plant stress status (Rouse et al. 1974; Huang et al. 2021). It exploits the tendency
580 of plants to reflect wavelengths of far and near-infrared light regardless of stress status while
581 increasingly reflecting wavelengths of visible light as stress becomes more severe (Ustin and
582 Jacquemoud 2020; Schepers et al. 1996). Prior to host-mediated selection, we performed
583 several preliminary experiments to confirm that NDVI values produced by our setup were
584 sensitive to changes in rice drought stress status over time (**Supplemental Figure 2**). We
585 confirmed that NDVI decreased with increasing drought stress and also showed that NDVI
586 highly correlated with rice percent water content (**Supplemental Figure 2D-E**).
587 To obtain NDVI values for plants, we first imaged them within a plywood lightbox
588 (**Supplemental Figures 2A, 4B**), the interior of which was painted with an ultra light-absorbing
589 black paint Culture Hustle USA, Black 3.0); all exterior corners sealed to ensure no light
590 contamination while full spectrum and far red (730nm) LED strips served as light sources within
591 the box (LEDLightsWorld, full spectrum: HK-CRI95F5050X30-X-6, 730nm: 5M-HK-8MM-F2835-
592 735-30-NW-IR-12). Two cameras simultaneously imaged plants, one a standard DSLR (Canon,
593 EOS Rebel T7), the other a DSLR modified to be able to detect red and infrared light (Canon,
594 EOS Rebel T1i) (**Supplemental Figure 2A-B**). Both cameras were set to: shutter speed = 1/40;
595 F-stop = 4.5; ISO = 100; Effect = Neutral; White balance = 7000K; Auto lighting optimizer =
596 OFF. The modified camera had previously been sent to LifePixel (Life Pixel Infrared; Mukilteo,
597 USA) where the factory infrared sensor filter was replaced by a dual-pass filter with high
598 transmission from 400-600nm and 700-800nm and complete out of band blocking.

Consequently, both cameras assign green and blue values near-equivalently, but have non-overlapping perceptions of red (**Supplemental Figure 2C**).

Paired images were then passed through a custom pipeline to derive NDVI. In particular, we relied heavily on tools from PlantCV (Fahlgren et al. 2015). All scripts are available on GitHub (github.com/colemanderr-lab/Styer-2024). In brief, we used a small section of black background to standardize all images by subtracting the median RGB values within that window from all pixels. Then, we used naive Bayes classifiers—previously trained on images from each camera—to segment plants from background; individual plants were then identified via object detection in the resultant binary mask and saved as separate images. We then extracted color data from each plant, including median red, green, and blue pixel intensities. Using these data from each set of paired images we calculated NDVI as the sum of median red values for both modified (MOD) and standard (STD) cameras divided by their difference:

$$NDVI = \frac{MOD_{red} + STD_{red}}{MOD_{red} - STD_{red}}$$

We then calculated the area under the curve of NDVI (AUC NDVI) for each plant by fitting a smoothed spline to NDVI values across the 10 days of drought; this allowed us to evaluate cumulative drought performance in a single metric. Lastly, because NDVI and plant biomass were anticorrelated (**Supplemental Figure 12**), we adjusted AUC NDVI by shoot dry weight biomass.

Selection scheme

Selections were made independently for each selection line and were determined by both fresh weight and NDVI. As a first filter, microbiomes were only eligible for selection if the fresh weight of their host plant was equal to or greater than the mean of the selection line. We set this initial filter to avoid selecting plants stunted by dysbiosis, having anticipated the negative correlation between NDVI and biomass but not yet having derived biomass-adjusted AUC NDVI values; without this initial filtering, we thought it possible, if not likely, selections based on NDVI alone would lead to the accumulation of pathogens. From the microbiomes that passed the biomass-based filter, we selected three from plants with the greatest cumulative NDVI score (i.e. the sum of daily NDVI values); these were then used to inoculate 15 plants to continue the selection line into a new generation. The two next best-performing microbiomes from each selection line were used to create inocula for the subsequent generation SI and LI control lines.

Inoculum preparation

For the enrichment generation (EG), we prepared inocula simply by mixing equal parts field soil (i.e. Rice Field, Desert, or Serpentine Seep) with sterilized calcined clay by weight. For sterile-inoculated lines, field soils were autoclaved in small batches for 90 minutes prior to mixing to ensure thorough sterilization. Calcined Clay soil treatment plants only received sterilized calcined clay as “inocula”. Pre-germinated rice plants were directly transplanted into the mixed substrates. The goal of the enrichment generation—during which no drought stress was applied—was to first enrich microbes that form associations with rice in non-stressed conditions. Endeavoring to minimize soil edaphic effects and to bias communities towards root-

641 associated bacteria, we only harvested roots and adhering soil—but not bulk soil—from
642 selected EG plants to inoculate the first selection generation (SG1).
643 To prepare selection generation inocula, we first shook roots to remove loosely adhering
644 soil, finely minced them with a sterile razor, then further macerated the collection with a mortar
645 and pestle. For SG1, the resultant root paste was thoroughly mixed into sterilized calcined clay
646 and rice plants directly transplanted into the inoculated substrate. For SG2 and later selection
647 generations, both root paste *and* bulk soil from selected plants were mixed into sterilized
648 calcined clay prior to rice transplantation. For each soil treatment, microbiomes selected to
649 inoculate SI and LI plants underwent the same preparation with the exception that the fraction
650 earmarked for SI was autoclave-sterilized prior to mixing with calcined clay.
651
652 ***16S rRNA library preparation***
653 At harvest, roots were shaken loose of soil, which, for droughted samples, amounted to
654 removing virtually all calcined clay particles. We did not further separate root rhizospheres from
655 endospheres and so we considered microbial community profiles collected from such samples
656 as "root associated." All roots were manipulated with clean gloves on sheets of single-use
657 aluminum foil; a portion of roots from each harvested plant were immediately placed in 15 ml
658 falcon tubes, flash frozen in liquid nitrogen, and stored at -80˚C. We later ground roots with
659 mortar and pestle in liquid nitrogen to prepare samples for DNA extraction. Approximately 0.1 g
660 of the resulting powder was added to Qiagen DNeasy 96 PowerSoil Pro kits and followed all
661 manufacturer's instructions to extract DNA (Qiagen, Hilden, Germany; catNo: 47017).
662 Next, we quantified extracted DNA (Invitrogen, Waltham, MA, USA; Quant-iT dsDNA
663 Assay Kit, CatNo. Q33120) and normalized all samples to equal concentrations prior to PCR. All
664 PCRs were performed in triplicate, each reaction consisting of 2uL DNA template at 5 ng/uL,
665 10uL PlatinumII Hot-Start PCR Master Mix (2x) plus 2uL GC-enhancer (Invitrogen, Waltham,
666 MA, USA; CatNo. 14000014), 0.19uL of 100uM mitochondrial PNA (GGCAAGTGTTCTTCGGA;
667 PNA Bio, Thousand Oaks, CA, USA; CatNo. MP01-50), 0.19uL of 100uM chloroplast PNA
668 (GGCTCAACCCTGGACAG; PNA Bio, Thousand Oaks, CA, USA; CatNo. PP01-50), 0.5uL of
669 10uM of each forward and reverse primer targeting the V3-V4 region of the 16S rRNA gene,
670 and water to bring final volume to 25uL. From 5'-3' complete primer sequences included an
671 Illumina adapter sequence, a 12 base pair index, an Illumina TruSeq primer sequence, a 1-7
672 base pair spacer to increase flow cell diversity, followed by forward
673 (CCTACGGGNBGCASCAG) and reverse (GACTACNVGGGTATCTAATCC) 16S rRNA primer
674 sequences; a complete list of primer sequences is available in **Supplemental Table 2**.
675 Thermocycling conditions were set to follow: an initial 3 min cycle at 94°C, then 36 cycles of 1
676 min at 94°C, 30 sec at 48°C, 1 min at 72°C, and a final cycle of 10 min at 72°C before holding at
677 4˚C indefinitely. Replicate PCRs were then pooled and quantified before pooling all libraries in
678 equimolar amounts. Pooled libraries were then cleaned with AMPure XP beads (Beckman
679 Coulter, Brea, CA, USA; CatNo. A63880) following the manufacturer's protocol, eluted in water,
680 then submitted to University of California, Berkeley's QB3 Genomics for Illumina MiSeq v3
681 300bp paired-end sequencing (Berkeley, CA, RRID:SCR_022170; Illumina, San Diego, CA,
682 USA).
683
684 ***16S rRNA sequence data processing***

685 Demultiplexed reads received from QB3 Genomics were imported into QIIME2 (Bolyen
686 et al. 2019) where primer sequences were removed using the Cutadapt plugin (Martin 2011).
687 Reads were then trimmed to remove low-quality base pair calls before being passed to the
688 DADA2 plugin (Callahan et al. 2016) for denoising and dereplication, resolving sequences into
689 amplicon sequence variants (ASVs). Representative sequences of ASVs were then assigned
690 taxonomies via the feature-classifier plugin (Bokulich et al. 2018) using the sklearn method
691 (Pedregosa et al. 2012) and a classifier trained on the SILVA 138 SSU Ref NR 99 16s rRNA
692 reference database (Quast et al. 2013). Lastly, prior to downstream analyses, we filtered ASVs
693 identified as either mitochondria or chloroplast and additionally removed any ASVs that were
694 observed in only one sample (out of 1425) and with fewer than five reads.
695
696 ***Shotgun metagenomic sequencing and analysis***
697 Thirty-seven samples were selected for shotgun metagenomic sequencing, each
698 representing a distinct Rice Field selection line at different time points spanning the seven
699 generations of the experiment. DNA was extracted from bulk soil combined from multiple plants
700 and extracted using Qiagen DNeasy 96 PowerSoil Pro kits following all manufacturer's
701 instructions (Qiagen, Hilden, Germany; catNo: 47017). All samples were then prepared by
702 Novogene (Novogene Corporation Inc., Sacramento, CA, USA) as 150bp paired-end libraries
703 and sequenced the Illumina NovaSeq platform, yielding an average 111 million reads per
704 library. Reads from each library were individually assembled *de novo* using MEGAHIT (D. Li et
705 al. 2015, 2016). Next, reads from each library were aligned to the accompanying assembly via
706 BWA-MEM (H. Li 2013). Three separate binning approaches: CONCOCT (Alneberg et al.
707 2014), MaxBin 2.0 (Wu, Simmons, and Singer 2016), and MetaBAT2 (Kang et al. 2019) using
708 both covariant tetranucleotide frequencies were applied to each library. Resultant bin sets were
709 combined and refined from these three approaches to produce a single set of high quality bins
710 using DAS Tool (Sieber et al. 2018). Bins from all libraries were subsequently combined and de-
711 replicated with dRep (Olm et al. 2017) to create a final set of metagenome-assembled genomes
712 (MAGs). Removing MAGs with >10% estimated contamination from other taxa and <70%
713 genome completion based on collocated sets of genes that are ubiquitous and single-copy
714 within a phylogenetic lineage (Lee 2019) yielded a final set of 272 high quality MAGs. Each
715 MAG was assigned taxonomic classification using GTDB-tk (Chaumeil et al. 2022). Finally
716 protein coding sequences were identified with prokka (Seemann 2014) and annotated
717 functionally using eggnog-mapper (Cantalapiedra et al. 2021). MAGs were manually assigned
718 to ASVs from the 16S amplicon sequencing analysis using both closest taxonomic matches and
719 comparing ASV and MAG abundances. In total, 165 MAGs were matched to ASVs.
720 In order to test for microbial functions associated with selected plant phenotypes, we
721 assessed the gene content of ASV-matched MAGs assigned to balance numerators for both
722 NDVI and Dry Weight plant phenotypes. We applied the hypergeometric test to identify
723 functional enrichments within these balance numerators relative to the background of all 165
724 ASV-matched MAGs. In the first round, we tested COG categories (Galperin et al. 2021).
725 Briefly, all genes in the numerator MAGs were grouped and tested for enrichment of genes in
726 each COG category relative to the background of the genes among all 165 ASV-matched MAGs
727 using the hypergeometric test as implemented in 'fgsea' (Korotkevich et al. 2016). In the second

round, we tested individual COGs among significantly enriched categories identified in the first round.

Data and code availability

Amplicon and shotgun metagenomic sequence data reported in this study are available in NCBI Bioproject PRJNA1067324. Scripts used to process images and analyze data are available on GitHub (github.com/colemanderr-lab/Styer-2024).

Acknowledgements

This research was supported by the National Aeronautics and Space Administration under the grant number NNX17AJ31G as well as by the United States Department of Agriculture ARS CRIS Grant 2030-12210-002-00D. This work was performed in part at the University of California Natural Reserve System McLaughlin Natural Reserve DOI: 10.21973/N3W08D. We appreciate insights from Ulrich Mueller that helped guide our initial experimental designs and thank Don Brubaker, Michael Derrico, Cathy Koehler, Kent McKenzie, Nicole Tautges, and Carrie Woods for their help facilitating soil collections. We also thank Ciana Caddell, Dawn Chiniquy, Citlali Fonseca-Garcia, Rachel Klaras, Bradie Lee, and Liana Ogden for their help harvesting and processing root samples. Lastly, thank you to Dan Naylor, Jen White, and Edi Wipf who provided helpful comments and suggestions prior to submission.

References

Adamberg, K., and S. Adamberg. 2018. “Selection of Fast and Slow Growing Bacteria from Fecal Microbiota Using Continuous Culture with Changing Dilution Rate.” *Microbial Ecology in Health and Disease* 29 (1): 1549922. https://doi.org/10.1080/16512235.2018.1549922.

Albareda, Marta, Dulce Nombre Rodríguez-Navarro, and Francisco J. Temprano. 2009. “Soybean Inoculation: Dose, N Fertilizer Supplementation and Rhizobia Persistence in Soil.” *Field Crops Research* 113 (3): 352–56. https://doi.org/10.1016/j.fcr.2009.05.013.

Alneberg, Johannes, Brynjar Smári Bjarnason, Ino de Bruijn, Melanie Schirmer, Joshua Quick, Umer Z. Ijaz, Leo Lahti, Nicholas J. Loman, Anders F. Andersson, and Christopher Quince. 2014. “Binning Metagenomic Contigs by Coverage and Composition.” *Nature Methods* 11 (11): 1144–46. https://doi.org/10.1038/nmeth.3103.

Anderson, Marti J., Thomas O. Crist, Jonathan M. Chase, Mark Vellend, Brian D. Inouye, Amy L. Freestone, Nathan J. Sanders, et al. 2011. “Navigating the Multiple Meanings of β Diversity: A Roadmap for the Practicing Ecologist.” *Ecology Letters* 14 (1): 19–28. https://doi.org/10.1111/j.1461-0248.2010.01552.x.

Aslam, Ana, Zahir Ahmad Zahir, Hafiz Naeem Asghar, and Muhammad Shahid. 2018. “Effect of Carbonic Anhydrase-Containing Endophytic Bacteria on Growth and Physiological Attributes of Wheat under Water-Deficit Conditions.” *Plant Production Science* 21 (3): 244–55. https://doi.org/10.1080/1343943X.2018.1465348.

Bååth, Erland. 1996. “Adaptation of Soil Bacterial Communities to Prevailing pH in Different Soils.” *FEMS Microbiology Ecology* 19 (4): 227–37. https://doi.org/10.1111/j.1574-6941.1996.tb00215.x.

Bell, Thomas. 2010. “Experimental Tests of the Bacterial Distance-Decay Relationship.” *The ISME Journal* 4 (11): 1357–65. https://doi.org/10.1038/ismej.2010.77.

Belotte, Dorothée, Jean-Baptiste Curien, R. Craig Maclean, and Graham Bell. 2003. “An

Experimental Test of Local Adaptation in Soil Bacteria." *Evolution; International Journal of Organic Evolution* 57 (1): 27–36. https://doi.org/10.1111/j.0014-3820.2003.tb00213.x.

Bilal, Lubna, Sajjad Asaf, Muhammad Hamayun, Humaira Gul, Amjad Iqbal, Ihsan Ullah, In-Jung Lee, and Anwar Hussain. 2018. "Plant Growth Promoting Endophytic Fungi Asprgillus Fumigatus TS1 and Fusarium Proliferatum BRL1 Produce Gibberellins and Regulates Plant Endogenous Hormones." *Symbiosis* 76 (2): 117–27. https://doi.org/10.1007/s13199-018-0545-4.

Bokulich, Nicholas A., Benjamin D. Kaehler, Jai Ram Rideout, Matthew Dillon, Evan Bolyen, Rob Knight, Gavin A. Huttley, and J. Gregory Caporaso. 2018. "Optimizing Taxonomic Classification of Marker-Gene Amplicon Sequences with QIIME 2's q2-Feature-Classifier Plugin." *Microbiome* 6 (1): 90. https://doi.org/10.1186/s40168-018-0470-z.

Bokulich, Nicholas A., John H. Thorngate, Paul M. Richardson, and David A. Mills. 2014. "Microbial Biogeography of Wine Grapes Is Conditioned by Cultivar, Vintage, and Climate." *Proceedings of the National Academy of Sciences of the United States of America* 111 (1): E139–48. https://doi.org/10.1073/pnas.1317377110.

Bolyen, Evan, Jai Ram Rideout, Matthew R. Dillon, Nicholas A. Bokulich, Christian C. Abnet, Gabriel A. Al-Ghalith, Harriet Alexander, et al. 2019. "Reproducible, Interactive, Scalable and Extensible Microbiome Data Science Using QIIME 2." *Nature Biotechnology* 37 (8): 852–57. https://doi.org/10.1038/s41587-019-0209-9.

Bradáčová, Klára, Andrea S. Florea, Asher Bar-Tal, Dror Minz, Uri Yermiyahu, Raneen Shawahna, Judith Kraut-Cohen, et al. 2019. "Microbial Consortia versus Single-Strain Inoculants: An Advantage in PGPM-Assisted Tomato Production?" *Agronomy* 9 (2): 105. https://doi.org/10.3390/agronomy9020105.

Burns, Adam R., W. Zac Stephens, Keaton Stagaman, Sandi Wong, John F. Rawls, Karen Guillemin, and Brendan Jm Bohannan. 2016. "Contribution of Neutral Processes to the Assembly of Gut Microbial Communities in the Zebrafish over Host Development." *The ISME Journal* 10 (3): 655–64. https://doi.org/10.1038/ismej.2015.142.

Callahan, Benjamin J., Paul J. McMurdie, Michael J. Rosen, Andrew W. Han, Amy Jo A. Johnson, and Susan P. Holmes. 2016. "DADA2: High-Resolution Sample Inference from Illumina Amplicon Data." *Nature Methods* 13 (7): 581–83. https://doi.org/10.1038/nmeth.3869.

Cantalapiedra, Carlos P., Ana Hernández-Plaza, Ivica Letunic, Peer Bork, and Jaime Huerta-Cepas. 2021. "eggNOG-Mapper v2: Functional Annotation, Orthology Assignments, and Domain Prediction at the Metagenomic Scale." *Molecular Biology and Evolution* 38 (12): 5825–29. https://doi.org/10.1093/molbev/msab293.

Chaumeil, Pierre-Alain, Aaron J. Mussig, Philip Hugenholtz, and Donovan H. Parks. 2022. "GTDB-Tk v2: Memory Friendly Classification with the Genome Taxonomy Database." *Bioinformatics* 38 (23): 5315–16. https://doi.org/10.1093/bioinformatics/btac672.

Chhetri, Geeta, Inhyup Kim, Minchung Kang, Jiyoun Kim, Yoonseop So, and Taegun Seo. 2022. "Devosia Rhizoryzae Sp. Nov., and Devosia Oryziradicis Sp. Nov., Novel Plant Growth Promoting Members of the Genus Devosia, Isolated from the Rhizosphere of Rice Plants." *Journal of Microbiology* 60 (1): 1–10. https://doi.org/10.1007/s12275-022-1474-8.

Chhetri, Geeta, Inhyup Kim, Minchung Kang, Yoonseop So, Jiyoun Kim, and Taegun Seo. 2022. "An Isolated Arthrobacter Sp. Enhances Rice (Oryza Sativa L.) Plant Growth." *Microorganisms* 10 (6). https://doi.org/10.3390/microorganisms10061187.

Debray, Reena, Robin A. Herbert, Alexander L. Jaffe, Alexander Crits-Christoph, Mary E. Power, and Britt Koskella. 2022. "Priority Effects in Microbiome Assembly." *Nature Reviews. Microbiology* 20 (2): 109–21. https://doi.org/10.1038/s41579-021-00604-w.

Delgado-Baquerizo, Manuel, Fernando T. Maestre, Peter B. Reich, Thomas C. Jeffries, Juan J. Gaitan, Daniel Encinar, Miguel Berdugo, Colin D. Campbell, and Brajesh K. Singh. 2016. "Microbial Diversity Drives Multifunctionality in Terrestrial Ecosystems." *Nature*

Communications 7 (January): 10541. https://doi.org/10.1038/ncomms10541.
De Sousa Fabiano Gama, Mielke Kamila Cabral, Marques Caldeira Dany Roberta, Divan Baldani Vera Lucia, Baldani Jose Ivo, da Silva Roberlan Ferreira, Balbinot Ernando, and Klein Vanderley Antonio Chorobura. 2022. "Genetic Diversity and Inoculation of Plant-Growth Promoting Diazotrophic Bacteria for Production of 'Eucalyptus Urophylla' Seedlings." *Australian Journal of Crop Science* 16 (1): 35–44. https://doi.org/10.3316/informit.643092702441833.
Díaz-García, Laura, Sixing Huang, Cathrin Spröer, Rocío Sierra-Ramírez, Boyke Bunk, Jörg Overmann, and Diego Javier Jiménez. 2021. "Dilution-to-Stimulation/Extinction Method: A Combination Enrichment Strategy To Develop a Minimal and Versatile Lignocellulolytic Bacterial Consortium." *Applied and Environmental Microbiology* 87 (2). https://doi.org/10.1128/AEM.02427-20.
Durrant, W. E., and X. Dong. 2004. "Systemic Acquired Resistance." *Annual Review of Phytopathology* 42: 185–209. https://doi.org/10.1146/annurev.phyto.42.040803.140421.
Evans, Sarah, Jennifer B. H. Martiny, and Steven D. Allison. 2017. "Effects of Dispersal and Selection on Stochastic Assembly in Microbial Communities." *The ISME Journal* 11 (1): 176–85. https://doi.org/10.1038/ismej.2016.96.
Fahlgren, Noah, Maximilian Feldman, Malia A. Gehan, Melinda S. Wilson, Christine Shyu, Douglas W. Bryant, Steven T. Hill, et al. 2015. "A Versatile Phenotyping System and Analytics Platform Reveals Diverse Temporal Responses to Water Availability in Setaria." *Molecular Plant* 8 (10): 1520–35. https://doi.org/10.1016/j.molp.2015.06.005.
Fan, Di, and Donald L. Smith. 2022. "Mucilaginibacter Sp. K Improves Growth and Induces Salt Tolerance in Nonhost Plants via Multilevel Mechanisms." *Frontiers in Plant Science* 13 (June): 938697. https://doi.org/10.3389/fpls.2022.938697.
Faust, Karoline, and Jeroen Raes. 2012. "Microbial Interactions: From Networks to Models." *Nature Reviews. Microbiology* 10 (8): 538–50. https://doi.org/10.1038/nrmicro2832.
Fierer, Noah, and Robert B. Jackson. 2006. "The Diversity and Biogeography of Soil Bacterial Communities." *Proceedings of the National Academy of Sciences of the United States of America* 103 (3): 626–31. https://doi.org/10.1073/pnas.0507535103.
Finkel, Omri M., Gabriel Castrillo, Sur Herrera Paredes, Isai Salas González, and Jeffery L. Dangl. 2017. "Understanding and Exploiting Plant Beneficial Microbes." *Current Opinion in Plant Biology* 38 (August): 155–63. https://doi.org/10.1016/j.pbi.2017.04.018.
Fitzpatrick, Connor R., Julia Copeland, Pauline W. Wang, David S. Guttman, Peter M. Kotanen, and Marc T. J. Johnson. 2018. "Assembly and Ecological Function of the Root Microbiome across Angiosperm Plant Species." *Proceedings of the National Academy of Sciences of the United States of America* 115 (6): E1157–65. https://doi.org/10.1073/pnas.1717617115.
Fodelianakis, Stilianos, Alexander Lorz, Adriana Valenzuela-Cuevas, Alan Barozzi, Jenny Marie Booth, and Daniele Daffonchio. 2019. "Dispersal Homogenizes Communities via Immigration Even at Low Rates in a Simplified Synthetic Bacterial Metacommunity." *Nature Communications* 10 (1): 1314. https://doi.org/10.1038/s41467-019-09306-7.
Franche, Claudine, Kristina Lindström, and Claudine Elmerich. 2009. "Nitrogen-Fixing Bacteria Associated with Leguminous and Non-Leguminous Plants." *Plant and Soil* 321 (1): 35–59. https://doi.org/10.1007/s11104-008-9833-8.
Frantz, Jonathan M., and Bruce Bugbee. 2002. "Anaerobic Conditions Improve Germination of a Gibberellic Acid Deficient Rice." *Crop Science* 42 (2): 651–54. https://doi.org/10.2135/cropsci2002.6510.
Friedman, Jonathan, Logan M. Higgins, and Jeff Gore. 2017. "Community Structure Follows Simple Assembly Rules in Microbial Microcosms." *Nature Ecology & Evolution* 1 (5): 109. https://doi.org/10.1038/s41559-017-0109.
Friesen, Maren L., Stephanie S. Porter, Scott C. Stark, Eric J. von Wettberg, Joel L. Sachs, and Esperanza Martinez-Romero. 2011. "Microbially Mediated Plant Functional Traits." *Annual*

Review of Ecology, Evolution, and Systematics 42 (1): 23–46. https://doi.org/10.1146/annurev-ecolsys-102710-145039.

Fukami, Josiane, Paula Cerezini, and Mariangela Hungria. 2018. “Azospirillum: Benefits That Go Far beyond Biological Nitrogen Fixation.” *AMB Express* 8 (1): 73. https://doi.org/10.1186/s13568-018-0608-1.

Galperin, Michael Y., Yuri I. Wolf, Kira S. Makarova, Roberto Vera Alvarez, David Landsman, and Eugene V. Koonin. 2021. “COG Database Update: Focus on Microbial Diversity, Model Organisms, and Widespread Pathogens.” *Nucleic Acids Research* 49 (D1): D274–81. https://doi.org/10.1093/nar/gkaa1018.

Garcia, Joshua, Maria Gannett, Liping Wei, Liang Cheng, Shengyuan Hu, Jed Sparks, James Giovannoni, and Jenny Kao-Kniffin. 2022. “Selection Pressure on the Rhizosphere Microbiome Can Alter Nitrogen Use Efficiency and Seed Yield in Brassica Rapa.” *Communications Biology* 5 (1): 959. https://doi.org/10.1038/s42003-022-03860-5.

Glick, Bernard R. 2005. “Modulation of Plant Ethylene Levels by the Bacterial Enzyme ACC Deaminase.” *FEMS Microbiology Letters* 251 (1): 1–7. https://doi.org/10.1016/j.femsle.2005.07.030.

Herrera Paredes, Sur, Tianxiang Gao, Theresa F. Law, Omri M. Finkel, Tatiana Mucyn, Paulo José Pereira Lima Teixeira, Isaí Salas González, et al. 2018. “Design of Synthetic Bacterial Communities for Predictable Plant Phenotypes.” *PLoS Biology* 16 (2): e2003962. https://doi.org/10.1371/journal.pbio.2003962.

Huang, Sha, Lina Tang, Joseph P. Hupy, Yang Wang, and Guofan Shao. 2021. “A Commentary Review on the Use of Normalized Difference Vegetation Index (NDVI) in the Era of Popular Remote Sensing.” *Research Journal of Forestry* 32 (1): 1–6. https://doi.org/10.1007/s11676-020-01155-1.

Johnson, Nancy Collins, Gail W. T. Wilson, Matthew A. Bowker, Jacqueline A. Wilson, and R. Michael Miller. 2010. “Resource Limitation Is a Driver of Local Adaptation in Mycorrhizal Symbioses.” *Proceedings of the National Academy of Sciences of the United States of America* 107 (5): 2093–98. https://doi.org/10.1073/pnas.0906710107.

Jones, Eric W., and Jean M. Carlson. 2019. “Steady-State Reduction of Generalized Lotka-Volterra Systems in the Microbiome.” *Physical Review. E* 99 (3-1): 032403. https://doi.org/10.1103/PhysRevE.99.032403.

Kalachova, Tetiana, Barbora Jindřichová, Lenka Burketová, Cécile Monard, Manuel Blouin, Samuel Jacquiod, Eric Ruelland, and Ruben Puga-Freitas. 2022. “Controlled Natural Selection of Soil Microbiome through Plant-Soil Feedback Confers Resistance to a Foliar Pathogen.” *Plant and Soil*, July. https://doi.org/10.1007/s11104-022-05597-w.

Kang, Dongwan D., Feng Li, Edward Kirton, Ashleigh Thomas, Rob Egan, Hong An, and Zhong Wang. 2019. “MetaBAT 2: An Adaptive Binning Algorithm for Robust and Efficient Genome Reconstruction from Metagenome Assemblies.” *PeerJ* 7 (July): e7359. https://doi.org/10.7717/peerj.7359.

Karmakar, Joydip, Sayani Goswami, Krishnendu Pramanik, Tushar Kanti Maiti, Rup Kumar Kar, and Narottam Dey. 2021. “Growth Promoting Properties of Mycobacterium and Bacillus on Rice Plants under Induced Drought.” *Plant Science Today* 8 (1): 49–57. https://doi.org/10.14719/pst.2021.8.1.965.

Kaur, Simranjit, Eleonora Egidi, Zhiguang Qiu, Catriona A. Macdonald, Jay Prakash Verma, Pankaj Trivedi, Juntao Wang, Hongwei Liu, and Brajesh K. Singh. 2022. “Synthetic Community Improves Crop Performance and Alters Rhizosphere Microbial Communities.” *Journal of Sustainable Agriculture and Environment* 1 (2): 118–31. https://doi.org/10.1002/sae2.12017.

King, William L., Laura M. Kaminsky, Maria Gannett, Grant L. Thompson, Jenny Kao-Kniffin, and Terrence H. Bell. 2022. “Soil Salinization Accelerates Microbiome Stabilization in Iterative Selections for Plant Performance.” *The New Phytologist* 234 (6): 2101–10.

https://doi.org/10.1111/nph.17774.
Korotkevich, Gennady, Vladimir Sukhov, Nikolay Budin, Boris Shpak, Maxim N. Artyomov, and Alexey Sergushichev. 2016. “Fast Gene Set Enrichment Analysis.” *bioRxiv*. bioRxiv. https://doi.org/10.1101/060012.
Kraemer, Susanne A., and Primrose J. Boynton. 2017. “Evidence for Microbial Local Adaptation in Nature.” *Molecular Ecology* 26 (7): 1860–76. https://doi.org/10.1111/mec.13958.
Kraemer, Susanne A., and Rees Kassen. 2015. “Patterns of Local Adaptation in Space and Time among Soil Bacteria.” *The American Naturalist* 185 (3): 317–31. https://doi.org/10.1086/679585.
Kramer, Jos, Özhan Özkaya, and Rolf Kümmerli. 2020. “Bacterial Siderophores in Community and Host Interactions.” *Nature Reviews. Microbiology* 18 (3): 152–63. https://doi.org/10.1038/s41579-019-0284-4.
Kumar, Akhilesh, Saurabh Singh, Anand Kumar Gaurav, Sudhakar Srivastava, and Jay Prakash Verma. 2020. “Plant Growth-Promoting Bacteria: Biological Tools for the Mitigation of Salinity Stress in Plants.” *Frontiers in Microbiology* 11 (July): 1216. https://doi.org/10.3389/fmicb.2020.01216.
Kuzyakov, Yakov, and Bahar S. Razavi. 2019. “Rhizosphere Size and Shape: Temporal Dynamics and Spatial Stationarity.” *Soil Biology & Biochemistry* 135 (August): 343–60. https://doi.org/10.1016/j.soilbio.2019.05.011.
Lee, Michael D. 2019. “GToTree: A User-Friendly Workflow for Phylogenomics.” *Bioinformatics* 35 (20): 4162–64. https://doi.org/10.1093/bioinformatics/btz188.
Li, Dinghua, Chi-Man Liu, Ruibang Luo, Kunihiko Sadakane, and Tak-Wah Lam. 2015. “MEGAHIT: An Ultra-Fast Single-Node Solution for Large and Complex Metagenomics Assembly via Succinct de Bruijn Graph.” *Bioinformatics* 31 (10): 1674–76. https://doi.org/10.1093/bioinformatics/btv033.
Li, Dinghua, Ruibang Luo, Chi-Man Liu, Chi-Ming Leung, Hing-Fung Ting, Kunihiko Sadakane, Hiroshi Yamashita, and Tak-Wah Lam. 2016. “MEGAHIT v1.0: A Fast and Scalable Metagenome Assembler Driven by Advanced Methodologies and Community Practices.” *Methods* 102 (June): 3–11. https://doi.org/10.1016/j.ymeth.2016.02.020.
Li, Heng. 2013. “Aligning Sequence Reads, Clone Sequences and Assembly Contigs with BWA-MEM.” *arXiv [q-bio.GN]*. arXiv. http://arxiv.org/abs/1303.3997.
Liu, Hongwei, Laura E. Brettell, Zhiguang Qiu, and Brajesh K. Singh. 2020. “Microbiome-Mediated Stress Resistance in Plants.” *Trends in Plant Science* 25 (8): 733–43. https://doi.org/10.1016/j.tplants.2020.03.014.
Liu, Hongwei, Zhiguang Qiu, Jun Ye, Jay Prakash Verma, Jiayu Li, and Brajesh K. Singh. 2022. “Effective Colonisation by a Bacterial Synthetic Community Promotes Plant Growth and Alters Soil Microbial Community.” *Journal of Sustainable Agriculture and Environment* 1 (1): 30–42. https://doi.org/10.1002/sae2.12008.
López, José L., Arista Fourie, Sanne W. M. Poppeliers, Nikolaos Pappas, Juan J. Sánchez-Gil, Ronnie de Jonge, and Bas E. Dutilh. 2023. “Growth Rate Is a Dominant Factor Predicting the Rhizosphere Effect.” *The ISME Journal* 17 (9): 1396–1405. https://doi.org/10.1038/s41396-023-01453-6.
Martin, Marcel. 2011. “Cutadapt Removes Adapter Sequences from High-Throughput Sequencing Reads.” *EMBnet.journal* 17 (1): 10–12. https://doi.org/10.14806/ej.17.1.200.
Martino, Cameron, James T. Morton, Clarisse A. Marotz, Luke R. Thompson, Anupriya Tripathi, Rob Knight, and Karsten Zengler. 2019. “A Novel Sparse Compositional Technique Reveals Microbial Perturbations.” *mSystems* 4 (1). https://doi.org/10.1128/mSystems.00016-19.
McCarty, Nicholas S., and Rodrigo Ledesma-Amaro. 2019. “Synthetic Biology Tools to Engineer Microbial Communities for Biotechnology.” *Trends in Biotechnology* 37 (2): 181–97. https://doi.org/10.1016/j.tibtech.2018.11.002.

Morton, James T., Jon Sanders, Robert A. Quinn, Daniel McDonald, Antonio Gonzalez, Yoshiki Vázquez-Baeza, Jose A. Navas-Molina, et al. 2017. “Balance Trees Reveal Microbial Niche Differentiation.” *mSystems* 2 (1). https://doi.org/10.1128/mSystems.00162-16.

Mueller, U. G., and J. L. Sachs. 2015. “Engineering Microbiomes to Improve Plant and Animal Health.” *Trends in Microbiology* 23 (10): 606–17. https://doi.org/10.1016/j.tim.2015.07.009.

Mueller, Ulrich G., and Timothy A. Linksvayer. 2022. “Microbiome Breeding: Conceptual and Practical Issues.” *Trends in Microbiology*, May. https://doi.org/10.1016/j.tim.2022.04.003.

Naylor, Dan, Stephanie DeGraaf, Elizabeth Purdom, and Devin Coleman-Derr. 2017. “Drought and Host Selection Influence Bacterial Community Dynamics in the Grass Root Microbiome.” *The ISME Journal* 11 (12): 2691–2704. https://doi.org/10.1038/ismej.2017.118.

Niu, Ben, Joseph Nathaniel Paulson, Xiaoqi Zheng, and Roberto Kolter. 2017. “Simplified and Representative Bacterial Community of Maize Roots.” *Proceedings of the National Academy of Sciences of the United States of America* 114 (12): E2450–59. https://doi.org/10.1073/pnas.1616148114.

Niu, Shuqi, Yan Gao, Huixian Zi, Ying Liu, Xuanming Liu, Xianqiu Xiong, Qingqing Yao, et al. 2022. “The Osmolyte-Producing Endophyte Streptomyces Albidoflavus OsiLf-2 Induces Drought and Salt Tolerance in Rice via a Multi-Level Mechanism.” *The Crop Journal* 10 (2): 375–86. https://doi.org/10.1016/j.cj.2021.06.008.

Olm, Matthew R., Christopher T. Brown, Brandon Brooks, and Jillian F. Banfield. 2017. “dRep: A Tool for Fast and Accurate Genomic Comparisons That Enables Improved Genome Recovery from Metagenomes through de-Replication.” *The ISME Journal* 11 (12): 2864–68. https://doi.org/10.1038/ismej.2017.126.

Orozco-Mosqueda, Ma Del Carmen, Gustavo Santoyo, and Bernard R. Glick. 2023. “Recent Advances in the Bacterial Phytohormone Modulation of Plant Growth.” *Plants* 12 (3). https://doi.org/10.3390/plants12030606.

Panda, Debabrata, Swati Sakambari Mishra, and Prafulla Kumar Behera. 2021. “Drought Tolerance in Rice: Focus on Recent Mechanisms and Approaches.” *Rice Science* 28 (2): 119–32. https://doi.org/10.1016/j.rsci.2021.01.002.

Pandey, Veena, and Alok Shukla. 2015. “Acclimation and Tolerance Strategies of Rice under Drought Stress.” *Rice Science* 22 (4): 147–61. https://doi.org/10.1016/j.rsci.2015.04.001.

Panke-Buisse, Kevin, Angela C. Poole, Julia K. Goodrich, Ruth E. Ley, and Jenny Kao-Kniffin. 2015. “Selection on Soil Microbiomes Reveals Reproducible Impacts on Plant Function.” *The ISME Journal* 9 (4): 980–89. https://doi.org/10.1038/ismej.2014.196.

Pedregosa, Fabian, Gaël Varoquaux, Alexandre Gramfort, Vincent Michel, Bertrand Thirion, Olivier Grisel, Mathieu Blondel, et al. 2012. “Scikit-Learn: Machine Learning in Python.” *arXiv [cs.LG]*. arXiv. https://www.jmlr.org/papers/volume12/pedregosa11a/pedregosa11a.pdf.

Pieterse, Corné M. J., Christos Zamioudis, Roeland L. Berendsen, David M. Weller, Saskia C. M. Van Wees, and Peter A. H. M. Bakker. 2014. “Induced Systemic Resistance by Beneficial Microbes.” *Annual Review of Phytopathology* 52 (June): 347–75. https://doi.org/10.1146/annurev-phyto-082712-102340.

Qian, Haoyu, Xiangchen Zhu, Shan Huang, Bruce Linquist, Yakov Kuzyakov, Reiner Wassmann, Kazunori Minamikawa, et al. 2023. “Greenhouse Gas Emissions and Mitigation in Rice Agriculture.” *Nature Reviews Earth & Environment* 4 (10): 716–32. https://doi.org/10.1038/s43017-023-00482-1.

Quast, Christian, Elmar Pruesse, Pelin Yilmaz, Jan Gerken, Timmy Schweer, Pablo Yarza, Jörg Peplies, and Frank Oliver Glöckner. 2013. “The SILVA Ribosomal RNA Gene Database Project: Improved Data Processing and Web-Based Tools.” *Nucleic Acids Research* 41 (Database issue): D590–96. https://doi.org/10.1093/nar/gks1219.

Richardson, Alan E., and Richard J. Simpson. 2011. “Soil Microorganisms Mediating

Phosphorus Availability Update on Microbial Phosphorus." *Plant Physiology* 156 (3): 989–96. https://doi.org/10.1104/pp.111.175448.

Rivas, Raúl, Anne Willems, Nanjappa S. Subba-Rao, Pedro F. Mateos, Frank B. Dazzo, Reiner M. Kroppenstedt, Eustoquio Martínez-Molina, Monique Gillis, and Encarna Velázquez. 2003. "Description of Devosia Neptuniae Sp. Nov. That Nodulates and Fixes Nitrogen in Symbiosis with Neptunia Natans, an Aquatic Legume from India." *Systematic and Applied Microbiology* 26 (1): 47–53. https://doi.org/10.1078/072320203322337308.

Rivera-Pinto, J., J. J. Egozcue, V. Pawlowsky-Glahn, R. Paredes, M. Noguera-Julian, and M. L. Calle. 2018. "Balances: A New Perspective for Microbiome Analysis." *mSystems* 3 (4). https://doi.org/10.1128/mSystems.00053-18.

Rodrigues, Elisete Pains, Luciana Santos Rodrigues, André Luiz Martinez de Oliveira, Vera Lucia Divan Baldani, Kátia Regina dos Santos Teixeira, Segundo Urquiaga, and Veronica Massena Reis. 2008. "Azospirillum Amazonense Inoculation: Effects on Growth, Yield and N2 Fixation of Rice (Oryza Sativa L.)." *Plant and Soil* 302 (1): 249–61. https://doi.org/10.1007/s11104-007-9476-1.

Rodríguez, Rodrigo, Patricio J. Barra, Giovanni Larama, Víctor J. Carrion, María de la Luz Mora, Lauren Hale, and Paola Durán. 2023. "Microbiome Engineering Optimized by Antarctic Microbiota to Support a Plant Host under Water Deficit." *Frontiers in Plant Science* 14 (September): 1241612. https://doi.org/10.3389/fpls.2023.1241612.

Rouse, John Wilson, Rüdiger H. Haas, John A. Schell, Donald W. Deering, and Others. 1974. "Monitoring Vegetation Systems in the Great Plains with ERTS." *NASA. Special Publication* 351 (1): 309. https://books.google.com/books?hl=en&lr=&id=e00CAAAAIAAJ&oi=fnd&pg=PA309&ots=JTTzbUCrWe&sig=fDJBu6FeoRGhZHIYk9mOevxqpo0.

Ruíz-Sánchez, Michel, Elisabet Armada, Yaumara Muñoz, Inés E. García de Salamone, Ricardo Aroca, Juan Manuel Ruíz-Lozano, and Rosario Azcón. 2011. "Azospirillum and Arbuscular Mycorrhizal Colonization Enhance Rice Growth and Physiological Traits under Well-Watered and Drought Conditions." *Journal of Plant Physiology* 168 (10): 1031–37. https://doi.org/10.1016/j.jplph.2010.12.019.

Russ, Dor, Connor R. Fitzpatrick, Paulo J. P. L. Teixeira, and Jeffery L. Dangl. 2023. "Deep Discovery Informs Difficult Deployment in Plant Microbiome Science." *Cell* 186 (21): 4496–4513. https://doi.org/10.1016/j.cell.2023.08.035.

Sansinenea, Estibaliz. 2019. "Bacillus Spp.: As Plant Growth-Promoting Bacteria." In *Secondary Metabolites of Plant Growth Promoting Rhizomicroorganisms: Discovery and Applications*, edited by Harikesh Bahadur Singh, Chetan Keswani, M. S. Reddy, Estibaliz Sansinenea, and Carlos García-Estrada, 225–37. Singapore: Springer Singapore. https://doi.org/10.1007/978-981-13-5862-3_11.

Santos-Medellín, Christian, Joseph Edwards, Zachary Liechty, Bao Nguyen, and Venkatesan Sundaresan. 2017. "Drought Stress Results in a Compartment-Specific Restructuring of the Rice Root-Associated Microbiomes." *mBio* 8 (4). https://doi.org/10.1128/mBio.00764-17.

Schepers, J. S., T. M. Blackmer, W. W. Wilhelm, and M. Resende. 1996. "Transmittance and Reflectance Measurements of CornLeaves from Plants with Different Nitrogen and Water Supply." *Journal of Plant Physiology* 148 (5): 523–29. https://doi.org/10.1016/S0176-1617(96)80071-X.

Schlatter, Daniel, Linda Kinkel, Linda Thomashow, David Weller, and Timothy Paulitz. 2017. "Disease Suppressive Soils: New Insights from the Soil Microbiome." *Phytopathology* 107 (11): 1284–97. https://doi.org/10.1094/PHYTO-03-17-0111-RVW.

Seemann, Torsten. 2014. "Prokka: Rapid Prokaryotic Genome Annotation." *Bioinformatics* 30 (14): 2068–69. https://doi.org/10.1093/bioinformatics/btu153.

Selim, Samy, Yasser M. Hassan, Ahmed M. Saleh, Talaat H. Habeeb, and Hamada AbdElgawad. 2019. "Actinobacterium Isolated from a Semi-Arid Environment Improves the

Drought Tolerance in Maize (Zea Mays L.).” *Plant Physiology and Biochemistry: PPB / Societe Francaise de Physiologie Vegetale* 142 (September): 15–21. https://doi.org/10.1016/j.plaphy.2019.06.029.

Sessitsch, Angela, Nikolaus Pfaffenbichler, and Birgit Mitter. 2019. “Microbiome Applications from Lab to Field: Facing Complexity.” *Trends in Plant Science* 24 (3): 194–98. https://doi.org/10.1016/j.tplants.2018.12.004.

Shayanthan, Ambihai, Patricia Ann C. Ordoñez, and Ivan John Oresnik. 2022. “The Role of Synthetic Microbial Communities (SynCom) in Sustainable Agriculture.” *Frontiers in Agronomy* 4. https://doi.org/10.3389/fagro.2022.896307.

Sieber, Christian M. K., Alexander J. Probst, Allison Sharrar, Brian C. Thomas, Matthias Hess, Susannah G. Tringe, and Jillian F. Banfield. 2018. “Recovery of Genomes from Metagenomes via a Dereplication, Aggregation and Scoring Strategy.” *Nature Microbiology* 3 (7): 836–43. https://doi.org/10.1038/s41564-018-0171-1.

Siebers, Meike, Mathias Brands, Vera Wewer, Yanjiao Duan, Georg Hölzl, and Peter Dörmann. 2016. “Lipids in Plant-Microbe Interactions.” *Biochimica et Biophysica Acta* 1861 (9 Pt B): 1379–95. https://doi.org/10.1016/j.bbalip.2016.02.021.

Sloan, William T., Mary Lunn, Stephen Woodcock, Ian M. Head, Sean Nee, and Thomas P. Curtis. 2006. “Quantifying the Roles of Immigration and Chance in Shaping Prokaryote Community Structure.” *Environmental Microbiology* 8 (4): 732–40. https://doi.org/10.1111/j.1462-2920.2005.00956.x.

Spaepen, Stijn. 2015. “Plant Hormones Produced by Microbes.” In *Principles of Plant-Microbe Interactions: Microbes for Sustainable Agriculture*, edited by Ben Lugtenberg, 247–56. Cham: Springer International Publishing. https://doi.org/10.1007/978-3-319-08575-3_26.

Spaepen, Stijn, and Jos Vanderleyden. 2011. “Auxin and Plant-Microbe Interactions.” *Cold Spring Harbor Perspectives in Biology* 3 (4). https://doi.org/10.1101/cshperspect.a001438.

Ustin, Susan L., and Stéphane Jacquemoud. 2020. “How the Optical Properties of Leaves Modify the Absorption and Scattering of Energy and Enhance Leaf Functionality.” In *Remote Sensing of Plant Biodiversity*, edited by Jeannine Cavender-Bares, John A. Gamon, and Philip A. Townsend, 349–84. Cham: Springer International Publishing. https://doi.org/10.1007/978-3-030-33157-3_14.

Vorholt, Julia A., Christine Vogel, Charlotte I. Carlström, and Daniel B. Müller. 2017. “Establishing Causality: Opportunities of Synthetic Communities for Plant Microbiome Research.” *Cell Host & Microbe* 22 (2): 142–55. https://doi.org/10.1016/j.chom.2017.07.004.

Wang, Boxi, and Shuichi Sugiyama. 2020. “Phylogenetic Signal of Host Plants in the Bacterial and Fungal Root Microbiomes of Cultivated Angiosperms.” *The Plant Journal: For Cell and Molecular Biology* 104 (2): 522–31. https://doi.org/10.1111/tpj.14943.

Wang, Honggui, Zhong Wei, Lijuan Mei, Jingxin Gu, Suisui Yin, Karoline Faust, Jeroen Raes, et al. 2017. “Combined Use of Network Inference Tools Identifies Ecologically Meaningful Bacterial Associations in a Paddy Soil.” *Soil Biology & Biochemistry* 105 (February): 227–35. https://doi.org/10.1016/j.soilbio.2016.11.029.

Weissman, J. L., Shengwei Hou, and Jed A. Fuhrman. 2021. “Estimating Maximal Microbial Growth Rates from Cultures, Metagenomes, and Single Cells via Codon Usage Patterns.” *Proceedings of the National Academy of Sciences of the United States of America* 118 (12). https://doi.org/10.1073/pnas.2016810118.

Whitham, Thomas G., Gerard J. Allan, Hillary F. Cooper, and Stephen M. Shuster. 2020. “Intraspecific Genetic Variation and Species Interactions Contribute to Community Evolution.” *Annual Review of Ecology, Evolution, and Systematics* 51 (1): 587–612. https://doi.org/10.1146/annurev-ecolsys-011720-123655.

Whitman, Thea, Rachel Neurath, Adele Perera, Ilexis Chu-Jacoby, Daliang Ning, Jizhong Zhou, Peter Nico, Jennifer Pett-Ridge, and Mary Firestone. 2018. “Microbial Community

Assembly Differs across Minerals in a Rhizosphere Microcosm." *Environmental Microbiology* 20 (12): 4444–60. https://doi.org/10.1111/1462-2920.14366.

Wright, Robyn J., Matthew I. Gibson, and Joseph A. Christie-Oleza. 2019. "Understanding Microbial Community Dynamics to Improve Optimal Microbiome Selection." *Microbiome* 7 (1): 85. https://doi.org/10.1186/s40168-019-0702-x.

Wu, Yu-Wei, Blake A. Simmons, and Steven W. Singer. 2016. "MaxBin 2.0: An Automated Binning Algorithm to Recover Genomes from Multiple Metagenomic Datasets." *Bioinformatics* 32 (4): 605–7. https://doi.org/10.1093/bioinformatics/btv638.

Xie, Li, and Wenying Shou. 2021. "Steering Ecological-Evolutionary Dynamics to Improve Artificial Selection of Microbial Communities." *Nature Communications* 12 (1): 6799. https://doi.org/10.1038/s41467-021-26647-4.

Xu, Ling, and Devin Coleman-Derr. 2019. "Causes and Consequences of a Conserved Bacterial Root Microbiome Response to Drought Stress." *Current Opinion in Microbiology* 49 (June): 1–6. https://doi.org/10.1016/j.mib.2019.07.003.

Xu, Ling, Zhaobin Dong, Dawn Chiniquy, Grady Pierroz, Siwen Deng, Cheng Gao, Spencer Diamond, et al. 2021. "Genome-Resolved Metagenomics Reveals Role of Iron Metabolism in Drought-Induced Rhizosphere Microbiome Dynamics." *Nature Communications* 12 (1): 3209. https://doi.org/10.1038/s41467-021-23553-7.

Xu, Ling, Dan Naylor, Zhaobin Dong, Tuesday Simmons, Grady Pierroz, Kim K. Hixson, Young-Mo Kim, et al. 2018. "Drought Delays Development of the Sorghum Root Microbiome and Enriches for Monoderm Bacteria." *Proceedings of the National Academy of Sciences of the United States of America* 115 (18): E4284–93. https://doi.org/10.1073/pnas.1717308115.

Xu, Peng, and Ertao Wang. 2023. "Diversity and Regulation of Symbiotic Nitrogen Fixation in Plants." *Current Biology: CB* 33 (11): R543–59. https://doi.org/10.1016/j.cub.2023.04.053.

Yandigeri, Mahesh S., Kamlesh Kumar Meena, Divya Singh, Nityanand Malviya, Dhananjaya P. Singh, Manoj Kumar Solanki, Arvind Kumar Yadav, and Dilip K. Arora. 2012. "Drought-Tolerant Endophytic Actinobacteria Promote Growth of Wheat (Triticum Aestivum) under Water Stress Conditions." *Plant Growth Regulation* 68 (3): 411–20. https://doi.org/10.1007/s10725-012-9730-2.

Zhang, Jingying, Weidong Liu, Jingshu Bu, Yanbing Lin, and Yang Bai. 2023. "Host Genetics Regulate the Plant Microbiome." *Current Opinion in Microbiology* 72 (April): 102268. https://doi.org/10.1016/j.mib.2023.102268.

Zhuang, Lubo, Yan Li, Zhenshuo Wang, Yue Yu, Nan Zhang, Chang Yang, Qingchao Zeng, and Qi Wang. 2021. "Synthetic Community with Six Pseudomonas Strains Screened from Garlic Rhizosphere Microbiome Promotes Plant Growth." *Microbial Biotechnology* 14 (2): 488–502. https://doi.org/10.1111/1751-7915.13640.

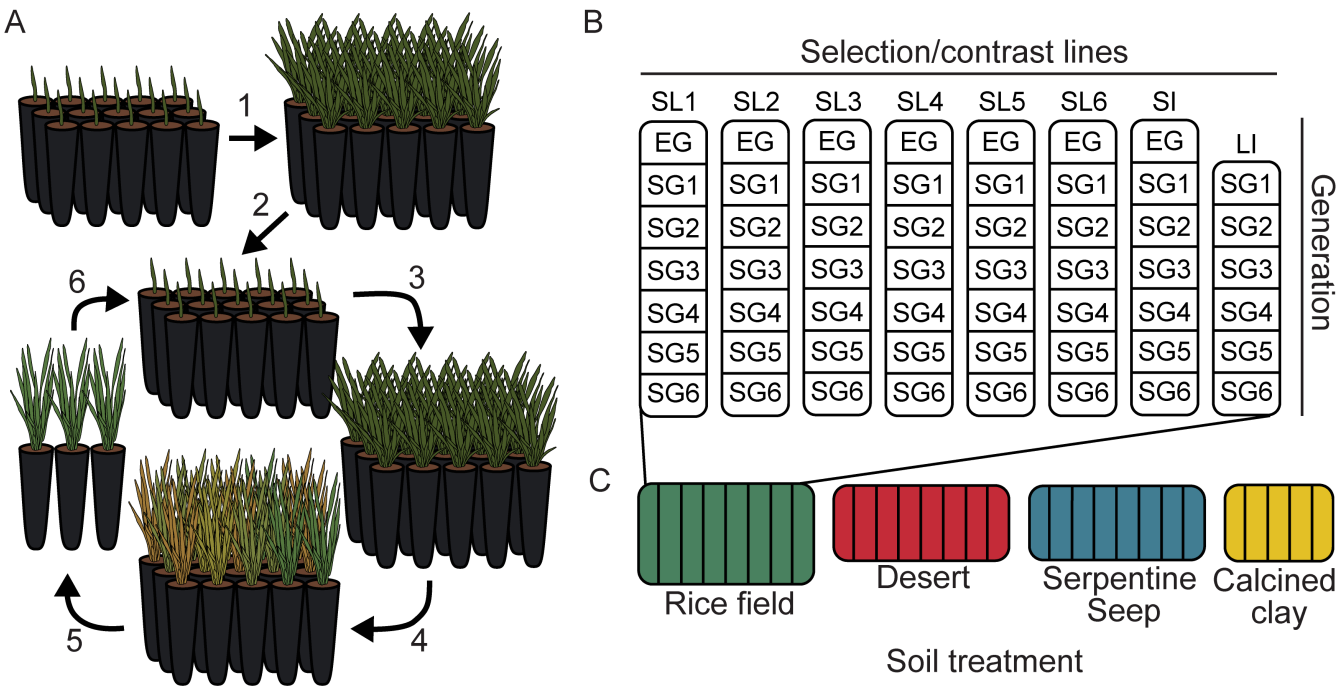

Figure 1. Host-mediated selection experimental design. (**A**) Representative of a single selection line of 15 rice plants. 1) Enrichment Generation (EG): rice are transplanted into 1:1 mixtures of field soil and sterilized calcined clay grow for 40 days in well-watered conditions. 2) Roots and adhering soil are harvested, minced, and ground, then mixed into sterilized calcined clay to inoculate the first selection generation (SG1). 3) SG plants grow for 30 days in well-watered conditions. 4) Drought treatment is initiated; plants are imaged daily to track phenotypes for 10 days. 5) The three best-performing plants are identified using Normalized Difference Vegetative Index (NDVI) and biomass data. 6) Roots and soils from best-performing plants are harvested and diluted with sterilized calcined clay to inoculate the subsequent selection generation (SG2). Steps 3-6 are then repeated iteratively for additional selection generations. (**B**) An overview of the type and number of selection and control lines for an individual soil treatment. Selection Lines (SL 1-6) consist of 15 plants per generation each and were maintained as independent lines across generations (i.e. transfers of selected inocula occurred within SLs). Sterile- and Live-Inoculated control lines (SI and LI), on the other hand, each included 30 plants per generation and were inoculated by an amalgam of material from all selection lines within their soil treatment; SI inocula were autoclave-sterilized prior to each generation. Like their SL counterparts, SI plants were well-watered throughout the enrichment generation and subjected to drought in selection generations; LI plants were well-watered in all generations. (**C**) Rice Field (green), Desert (red), and Serpentine Seep (blue) soil treatments—inoculated by field soils—each included six selection lines (SL 1-6) of 15 plants per generation. Calcined Clay (yellow) did not receive any inoculum in EG, instead assembling microbiomes composed of environmental taxa, and included just three SLs of 15 plants per generation. The number and length of columns are proportional to the number of lines and selection generations, respectively, associated with each soil treatment.

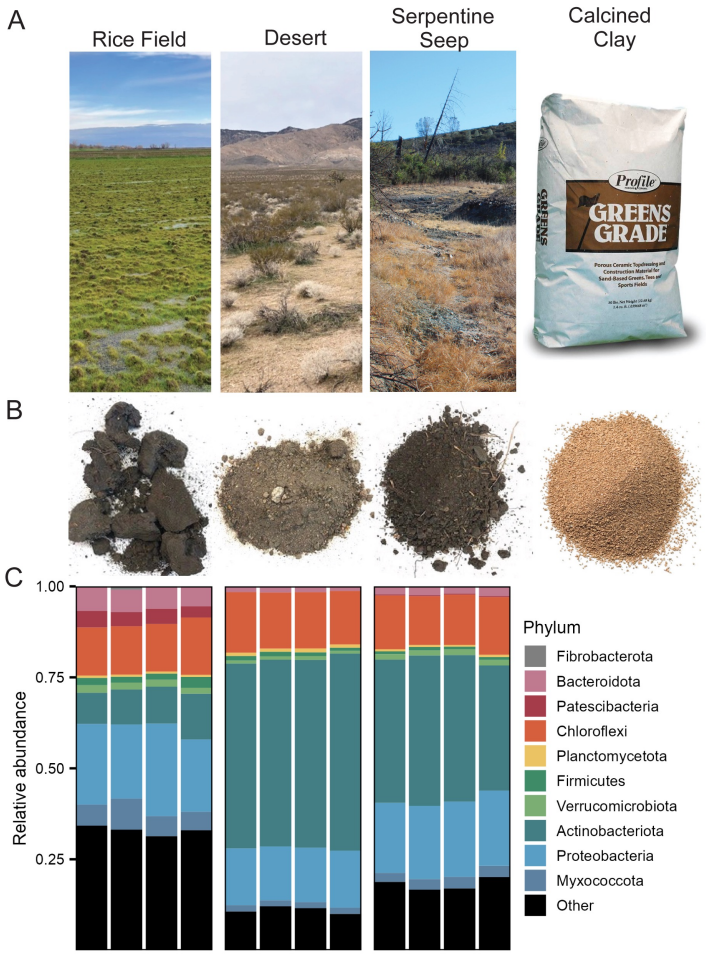

Figure 2. Field sites, soils, and starting diversity of source inocula. **(A)** Collection sites for Rice Field, Desert, and Serpentine Seep. Calcined Clay "source inocula" was simply calcined clay (Profile Greens Grade, Cat.No. FZ-TP) that was rinsed and autoclave-sterilized before use. **(B)** Field soils differed in physico-chemical characteristics (Supplemental Table 1). Rice Field was visibly clay-dominant, Desert predominantly sandy, and Serpentine Seep high in organic matter, but less clay-like compared to Rice Field. **(C)** Bacterial diversity and community compositions were distinct for each soil, even at broad taxonomic levels (Supplemental Figure 1).

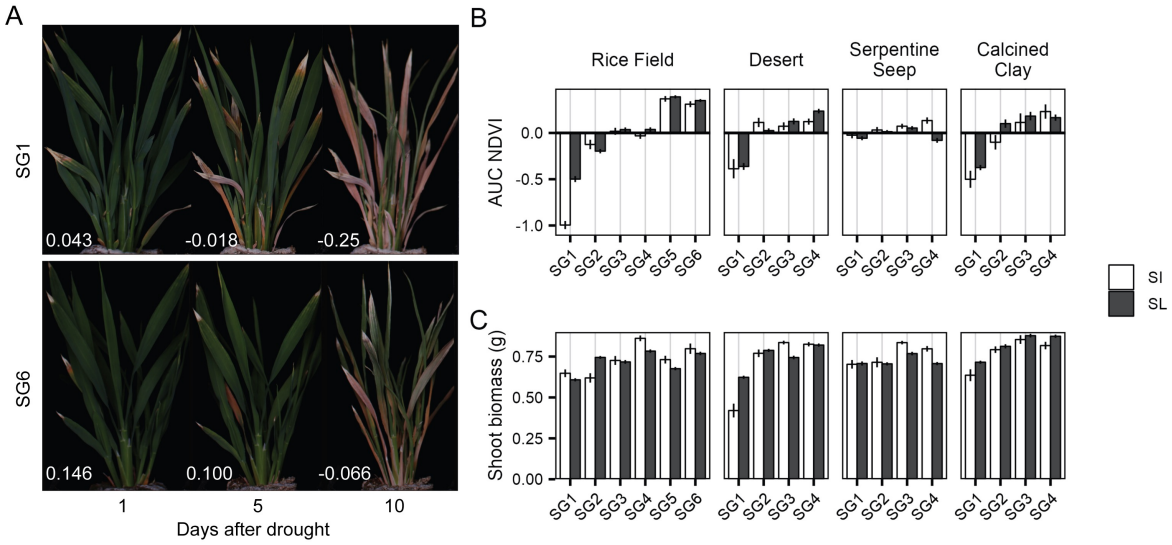

Figure 3. Rice phenotypes across host-mediated selection generations. (**A**) Representative images of Rice Field selection line plants in the first (SG1) and last (SG6) selection generations at 1, 5, and 10 days after drought. NDVI values are shown in the bottom left corner of each image. (**B**) Drought tolerance, quantified as the area under the curve of NDVI values (AUC NDVI), significantly improved for all soil treatments except Serpentine Seep. Here, we show data for all selection lines combined (gray bars) and assessed the response of AUC NDVI to generation via linear mixed effects models (formula = AUC NDVI ~ generation + (1|selection line); Rice Field: β=0.17, t = 28.8, p < 2e-16; Desert: β=0.19, t = 14.1, p < 2e-16; Serpentine Seep: β=-0.003, t = -0.3, p = NS; Calcined Clay: β=0.17, t = 8.7, p < 0.001). Filled bars represent the mean AUC NDVI value of all selection line (SL) plants +/- one standard error; white, unfilled bars are data for sterile-inoculated (SI) plants. Because selection lines were independent of one another, we also tested them individually via OLS regression: all selection lines of Rice Field (6/6), Desert (6/6), and Calcined Clay (3/3) significantly improved over time; Serpentine Seep included selection lines that both significantly improved (2/6) and worsened (2/6) (Supplemental Figure 3). (**C**) Shoot dry weight biomass also significantly increased across selection generations for all soil treatments, except Serpentine Seep (Rice Field: β=0.02, t =7.0, p < 2e-16; Desert: β=0.06, t =11.6, p < 2e-16; Serpentine Seep: β=0.006, t =1.2, p = NS; Calcined Clay: β=0.05, t =10.3, p < 2e-16). Tested individually, all selection lines of Rice Field (6/6) and Calcined Clay (3/3) significantly improved over time; most Desert selection lines (5/6) significantly improved; Serpentine Seep included one selection line that significantly increased (1/6) and one that significantly decreased (1/6) (Supplemental Figure 3).

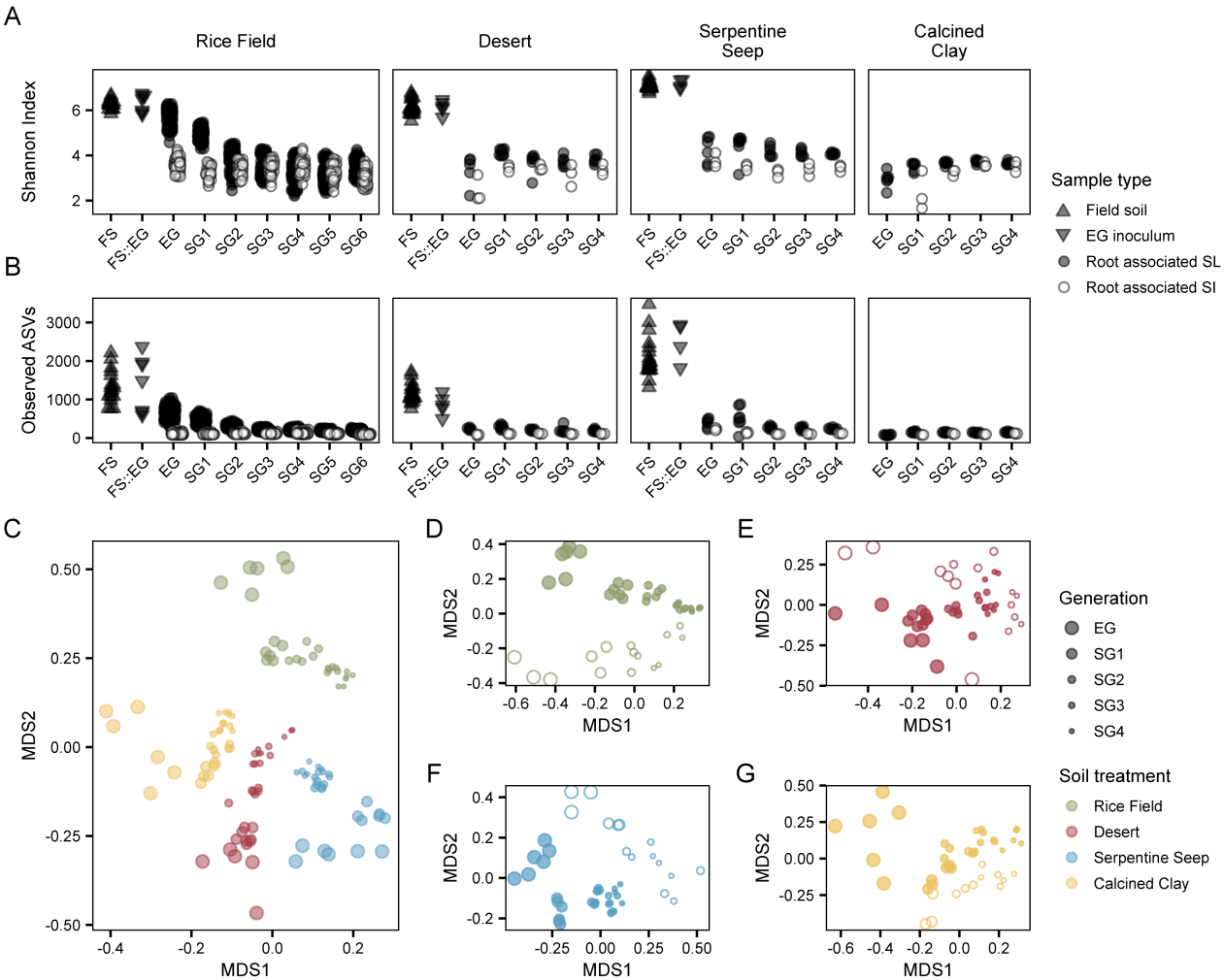

Figure 4. Alpha and beta diversity of bacterial communities over time. (**A**) Shannon-Index diversity and (**B**) number of observed ASVs for soil treatments over time. Each point represents a bacterial community from one of several sample types, including original field soils (FS), enrichment generation (EG) inocula (FS::EG), root-associated selection line (SL), or root associated sterile-inoculated (SI); sample types are indicated by shape. EG inocula were simply field soil diluted by sterilized calcined clay. Sample sizes and numbers of selection generations differ between soil treatments; having observed increasing similarities in microbiome composition between soil treatments after four selection generations, we decided to focus effort and resources on Rice Field, which we carried forward an additional two selection generations. (**C**) Bray-Curtis (BC) dissimilarity between soil treatment selection lines plotted in two-dimensional space. Each point represents an individual sample, where color indicates soil treatment and size indicates generation. BC values are the average of 1000 permutations where each sample was individually subset to 5000 reads. (**D-G**) Similar to (C), but panels are individual soil treatments and include both SL (filled) and SI (unfilled) samples. Despite forming distinct clusters, SL and SI microbiomes generally follow parallel compositional trajectories through time. For ordinations in panels C and D, Rice Field samples were subset to match the sequencing effort of other soil treatments prior to calculating BC values.

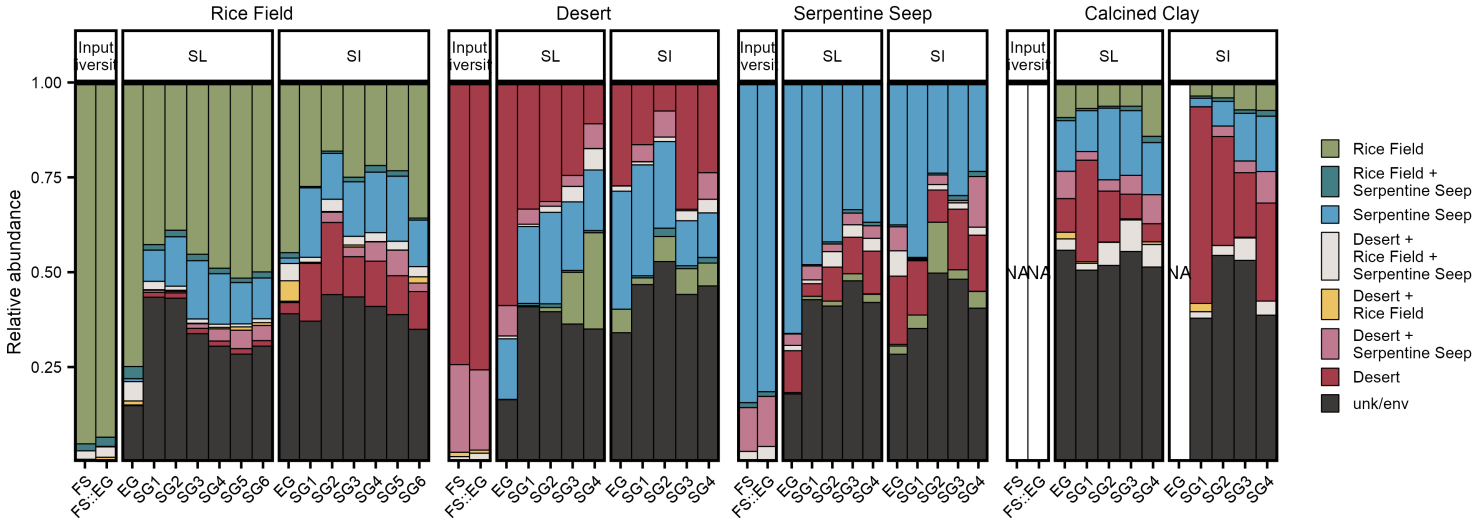

Figure 5. Dispersal homogenizes microbiomes over time. Using both original field soils (FS) and enrichment generation inocula (FS::EG, field soil mixed with sterile calcined clay), we assigned ASVs as originally belonging to one or multiple soil origins and is indicated by color. For example, if an ASV was observed in field soil or inocula samples for Rice Field, but not Desert or Serpentine Seep, it was designated a Rice Field ASV; if observed in Rice Field and Serpentine Seep, but not Desert, it was designated a “Rice Field + Serpentine Seep” ASV. ASVs that were not observed in either the field soil samples or source inocula were assigned “unk/env” to indicate their origin as unknown, but likely from the growth chamber environment.
Notably, sterile-inoculated (SI) lines of each soil treatment—which acquired microbiomes from the environment—were each biased towards their respective soil treatments. Calcined Clay, which received no initial inoculum in the enrichment generation was more evenly represented by ASVs from other soil treatments.

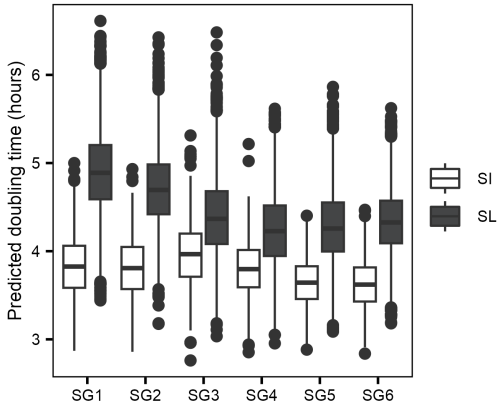

Figure 6. Microbiomes become overrepresented by fast-growing taxa over time. We determined ASV doubling times by matching ASVs to the Estimated Growth rates from gRodon Online (EGGO) database. We then performed 1000 bootstraps randomly subsetting 100 ASVs that were present in each generation for selection line (SL) and sterile-inoculated (SI) microbiomes. Each point represents the mean predicted doubling time of the ASV subset in each bootstrap. By setting generation as a numeric factor and performing OLS regression, we found that predicted doubling time significantly decreased across selection generations in both SL (t = -90.9, p<2e-16) and SI (t = -19.6, p<2e-16) samples.

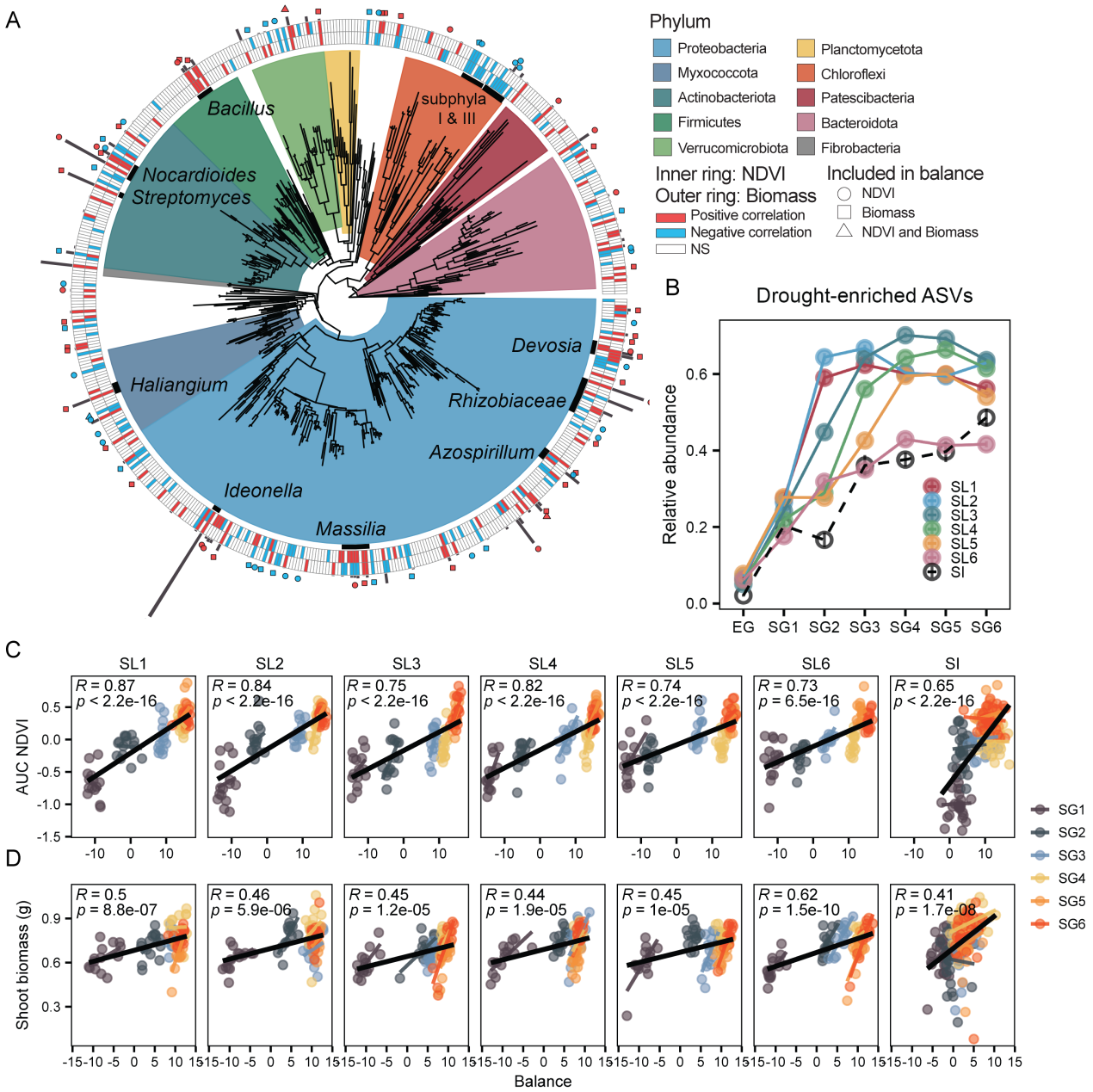

Figure 7. Identifying phenotype-associated ASVs. (**A**) A phylogeny of Rice Field ASVs remaining after four selection generations with branches colored by phylum; black bars and corresponding labels highlight notable clades at lower taxonomic levels. The inner (AUC NDVI) and outer (Shoot biomass) tiled rings indicate whether an ASV showed a strong positive (red) or negative (blue) response to phenotype, or lack thereof (white). To determine whether a response was strong or not, we ran two mixed effects linear models for each ASV-phenotype combination. One model included selection line as a random factor, while the other included selection generation as a random factor nested within selection line; doing so allowed us to better hone in on ASVs that were both enriched over time and consistently correlated with phenotypes within selection generations. Responses were considered strong if the t-value resulting from one or both models was two or more standard deviations away from the mean. Gray bars extending outward from the tiled rings indicate the median relative abundance of ASVs in the final selection generation (SG6). Symbols beyond the gray bars denote whether ASVs were included in the numerator (red) or denominator (blue) of the balances shown in panel C. (**B**) The mean, combined relative abundance of drought enriched ASVs over time; error bars (present, but small) are +/- one standard error of the mean. Drought enriched ASVs were identified using the effect and t-test functions in the ALDEx2 R package by comparing CLR-transformed abundances between SL (droughted) and LI (not droughted) plants at each selection generation. (**C**) Balances successfully predict NDVI and biomass phenotypes. In brief, balances are compositionally-aware log contrasts in which the numerator and denominator represent two sets of ASVs whose ratio can be used to predict a continuous phenotype (Rivera-Pinto et al. 2018). We composed distinct balances for each phenotype and performed OLS regressions on individual lines; in each case, SI lines included, balances were significant predictors of plant phenotype. Statistics and black trendlines correspond to the overall regression; colored trendlines show the relationship between balance values and phenotype within generations.

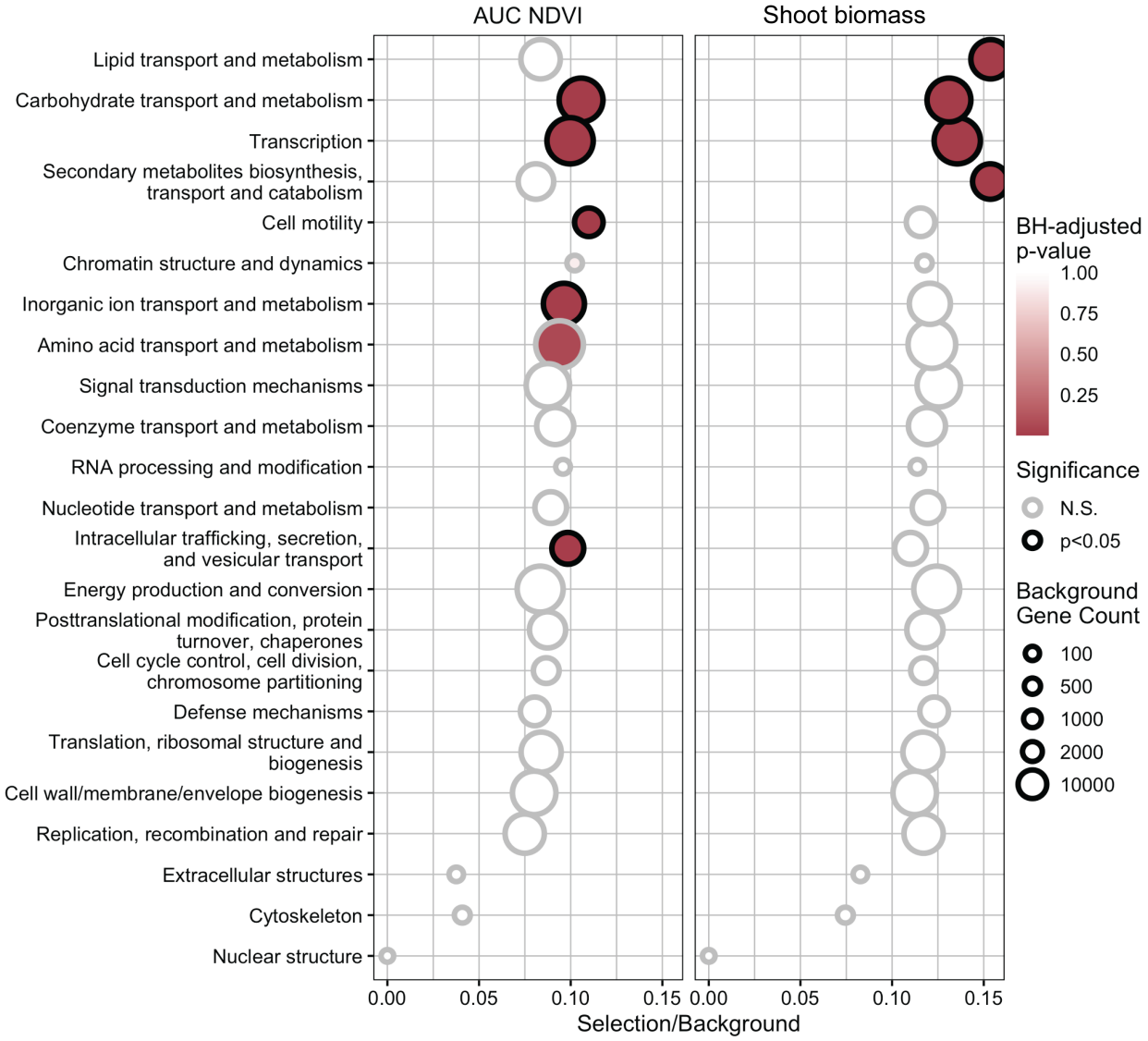

Figure 8. Bacterial communities associated with increased plant biomass and plant vigor during drought are enriched for both common and distinct functions. By comparing the metagenome-assembled genomes (MAGs) of taxa from balance group numerators with all other MAGs in the dataset, we identified high level functional categories that were significantly enriched in the genomes of these groups. Selection/Background refers to the ratio of gene counts among phenotype-associated taxa relative to all taxa for each functional category. The size of points indicates the background gene count, or the total number of genes within a functional category represented by all MAGs. We determined p-values with hypergeometric tests and applied multiple testing correction before determining significance. Functional categories that were significantly enriched in balance numerator groups were then further investigated to identify significantly enriched individual COGs (Supplemental Figures 10-11)

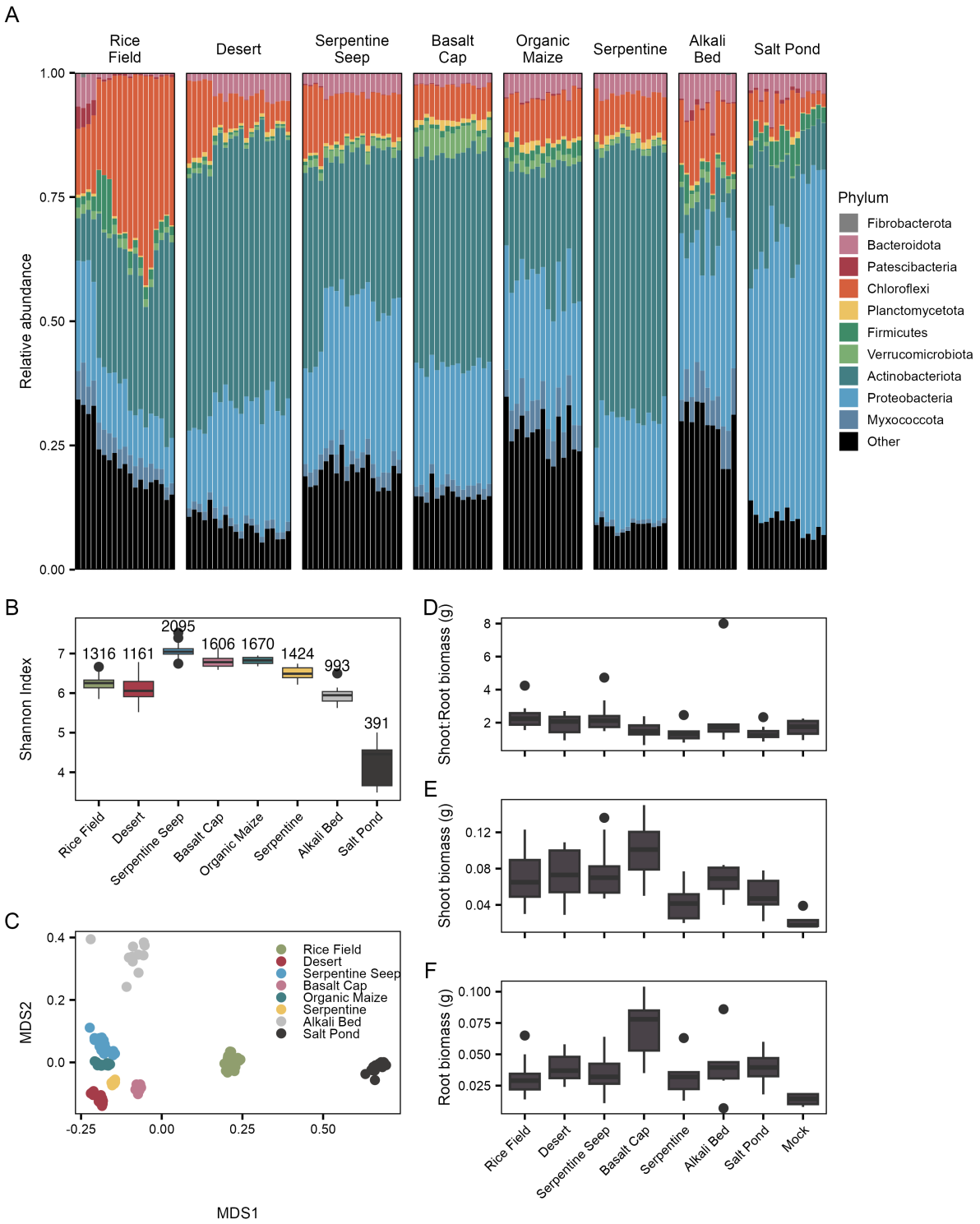

Supplemental Figure 1. Bacterial diversity of field soils collected as candidate source inocula for host-mediated selection. (**A**) Relative abundance barplots colored by Phylum show large differences between soil bacterial communities even at coarse taxonomic levels. Each bar represents an individual technical replicate. (**B**) Shannon-Index diversity for each soil. The mean number of observed ASVs are shown above each boxplot. (**C**) NMDS-ordinated Bray-Curtis dissimilarity between soils. (D-F) Phenotypic data from a pilot study where rice plants were either inoculated with the field soils shown in A-C or mock inoculated.

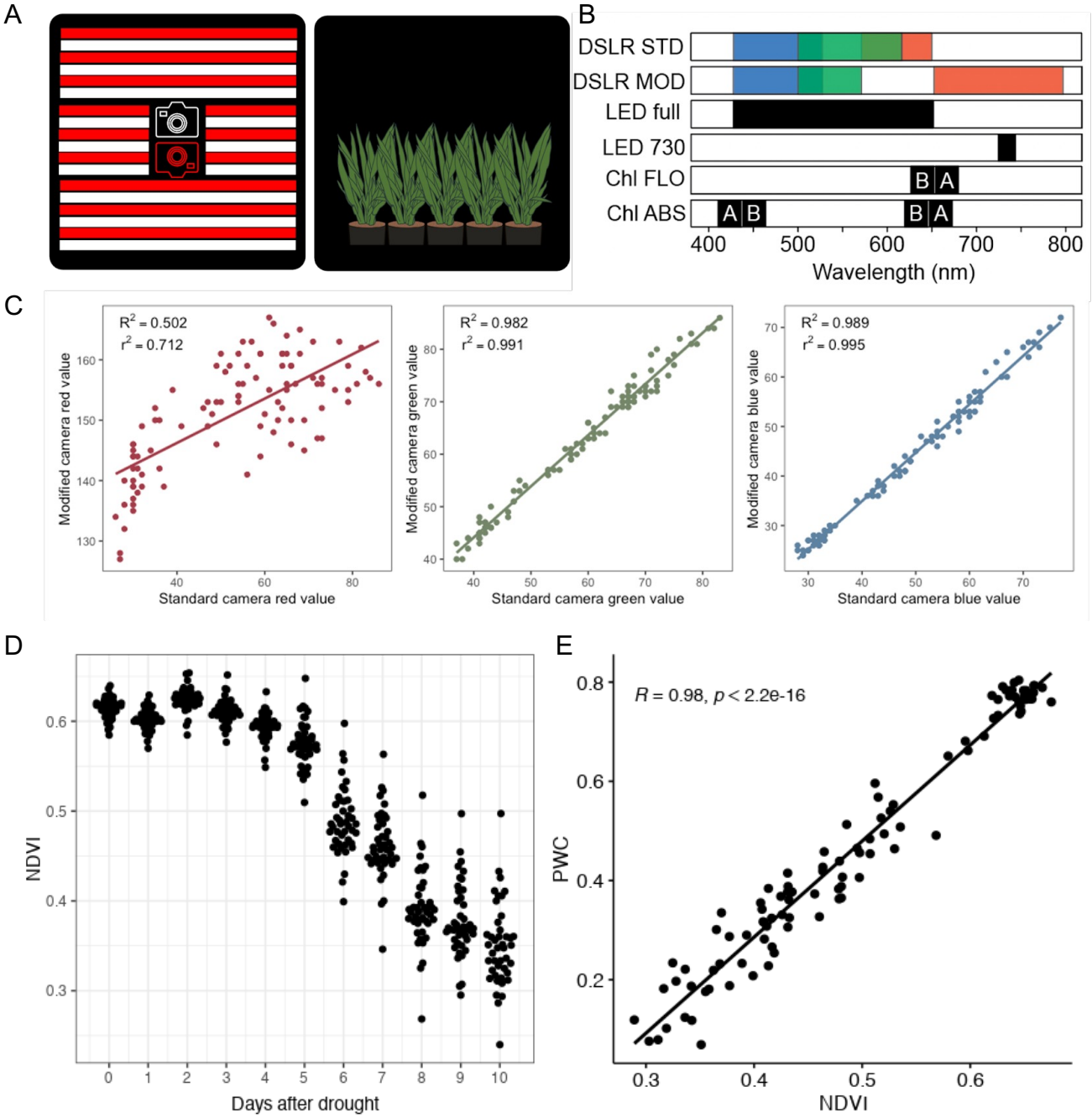

Supplemental Figure 2. (**A**) Simplified schematic of lightbox design depicting full spectrum (white) and 730nm (red) LED light strips as well as the position of the standard (white) and modified (red) cameras. The interior of the box was painted with an ultra light-absorbing black paint. A shared shutter trigger ensured images from both cameras were captured simultaneously; up to five plants were imaged at the same time. (**B**) A representative drawing of the portions of visible and near-infrared light each camera's red, green, and blue channels were sensitive to. Beneath, black bars indicate the range of emission spectra of light sources as well as wavelengths expected to be absorbed (ABS) and fluoresced (FLO) by chlorophyll. (**C**) Comparisons of the standard and modified cameras' median values for red, green, and blue channels individually; each dot represents an individual plant. (**D**) NDVI responds to rice drought stress status over time. Generally, the interval between two time points with the largest difference corresponds to the visible onset of leaf curling symptoms (data not shown). (**E**) At harvest, NDVI is highly predictive of rice percent water content.

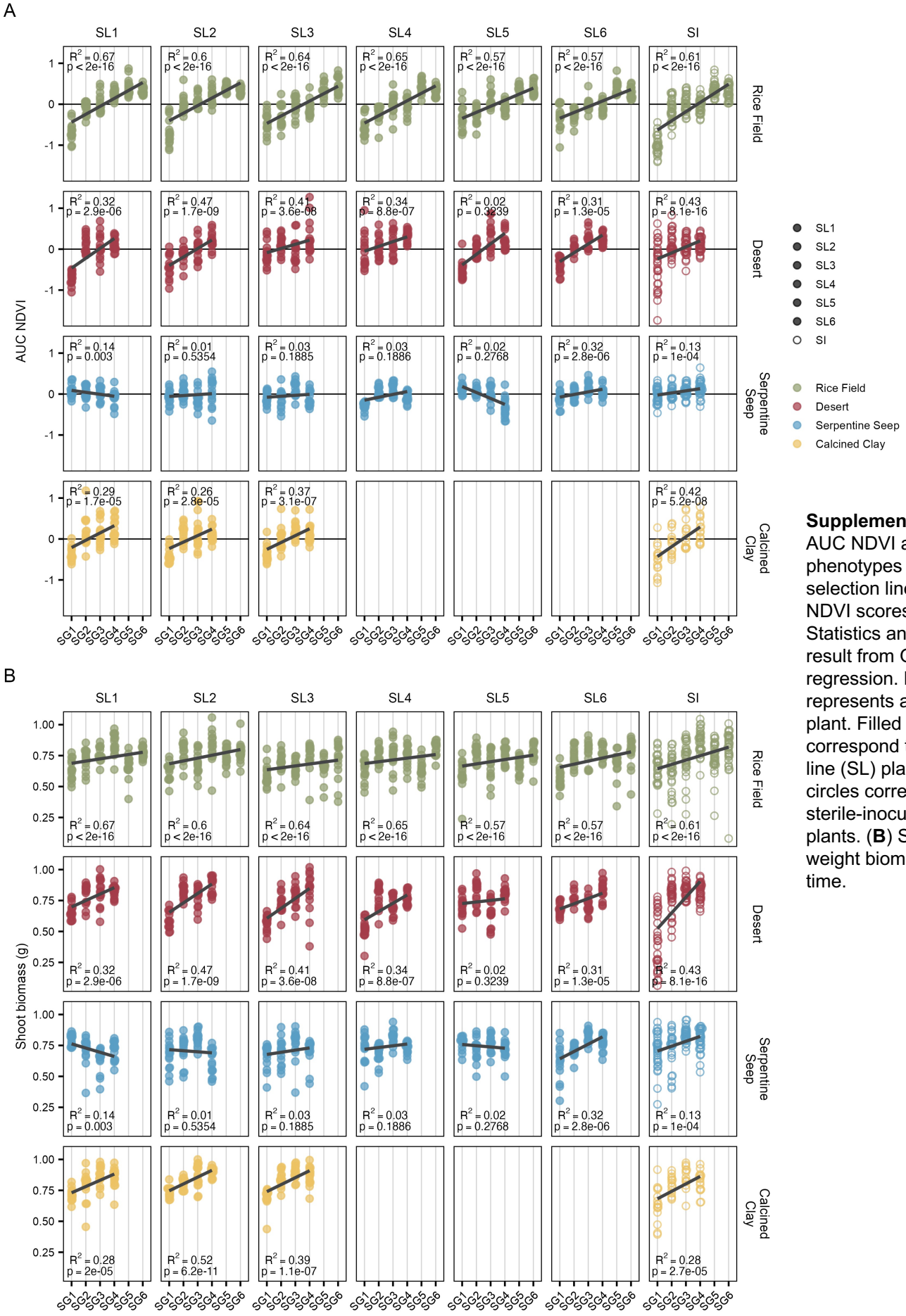

Supplemental Figure 3. AUC NDVI and biomass phenotypes for individual selection lines. (**A**) AUC NDVI scores over time. Statistics and trendlines result from OLS regression. Each point represents an individual plant. Filled circles correspond to selection line (SL) plants; open circles correspond to sterile-inoculated (SI) plants. (**B**) Shoot dry weight biomass over time.

Supplemental Figure 4. Rice growth conditions. (**A**) Rice were grown in spatially discrete conetainers and water reservoirs to minimize admixture of microbiomes. A small ball of polyester fiber was placed at the bottom of conetainers to prevent substrate from spilling out. Reservoirs were filled with milliQ water which calcined clay substrate was able to wick to the top surface of the container. (**B**) Host-mediated selection was performed in a walk-in growth chamber set to 16-hour days, during which daytime temperature and humidity were held at 28˚C and 80%, respectively, and relaxed to 24˚C and 75% humidity at night. Each soil treatment was grown on its own shelving unit, but plants were rotated within that unit every three days to ensure each plant experienced the same overall environment and ballast exposure. The lightbox with a rack of plants ready to be imaged can be seen in the bottom right corner.

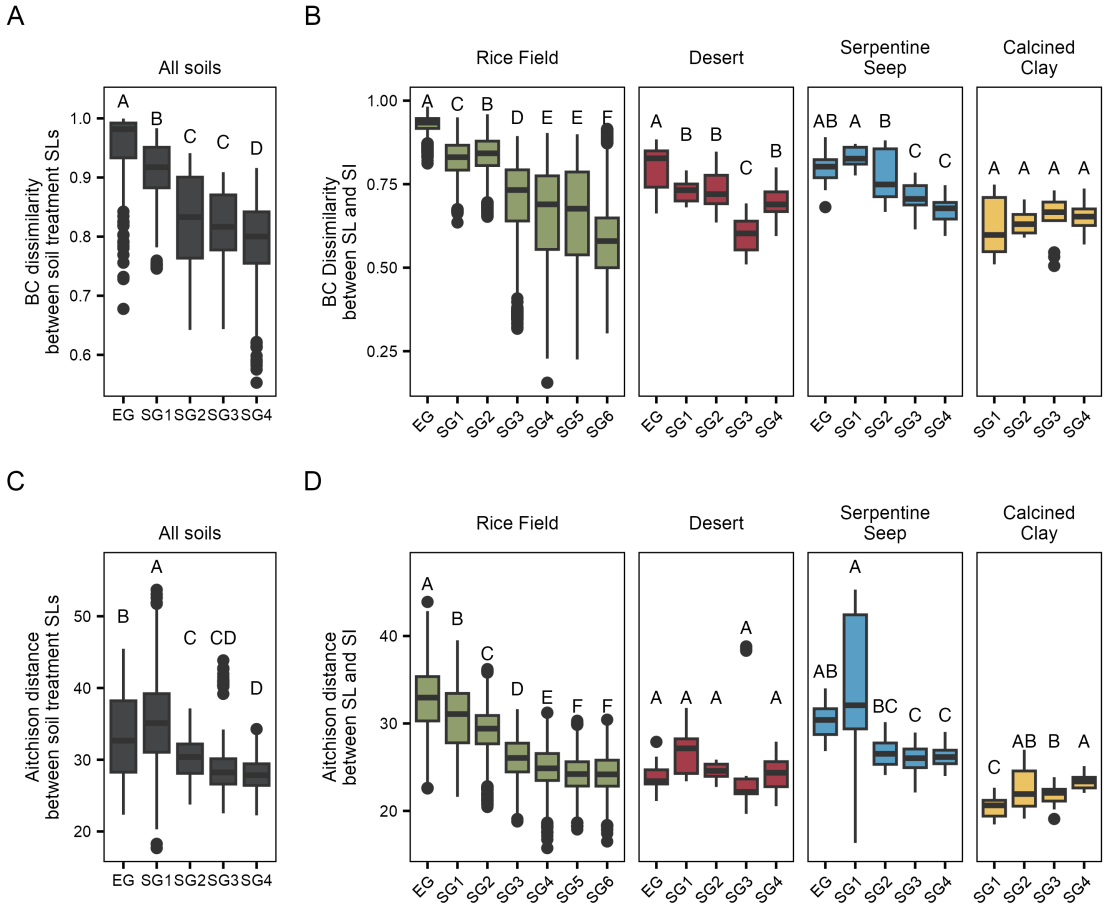

Supplemental Figure 5. Bray-Curtis dissimilarity (**A-B**) and Aitchison distance (**C-D**) between and within soil treatments across selection generations. Panels A and C show dissimilarity/distances between soil treatment selection lines by BC dissimilarity and Aitchison distance, respectively. Panels B and E are similar, except dissimilarity/distance is between selection line and steril-inoculated microbiomes within soil treatments. BC values are the average of 1000 permutations where each sample was individually subset to 5000 reads. Aitchison distance was calculated as the Euclidean distance between samples after read counts were transformed via robust centered log ratio transformation. Letters above boxplots are the result of a post-hoc Tukey HSD with 95% confidence intervals ($p<0.05$) to detect significant differences between groups. Rice Field samples were subset to match the sequencing effort of other soil treatments when generating data for panels A and C.

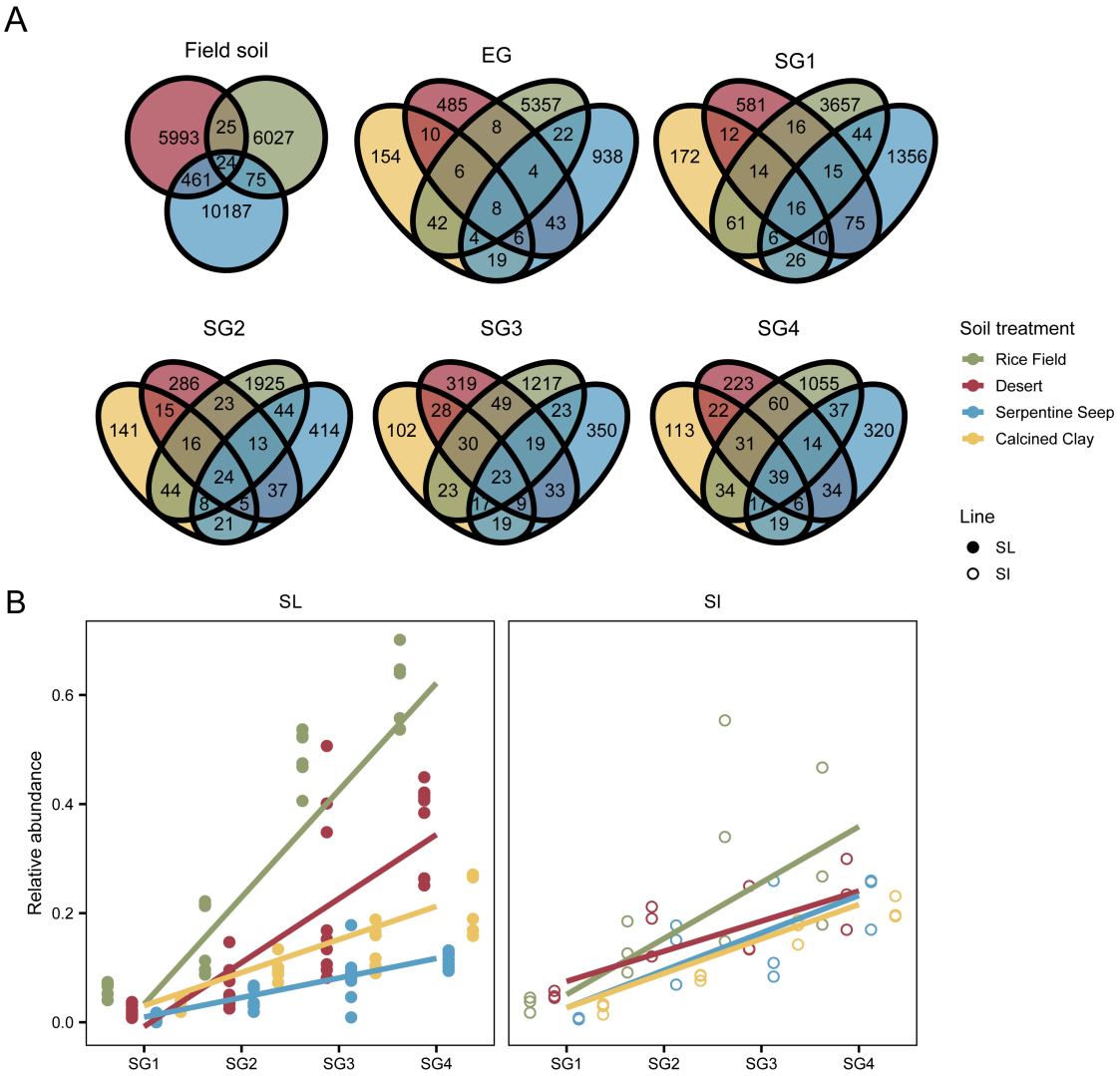

Supplemental Figure 6. The number and abundance of ASVs shared between soil treatments increased over time. (**A**) Venn diagrams for the numbers of ASVs shared between soil treatments at each generation. Venn components are colored by soil treatment: Rice Field (green), Desert (red), Serpentine Seep (blue), and Calcined Clay (yellow). (**B**) The combined relative abundance of the top 20 ASVs commonly enriched in all soil treatments over time. Each point represents an individual sample. Patterns of enrichment were similar for both selection line (filled circles) and sterile-inoculated (open circles) microbiomes.

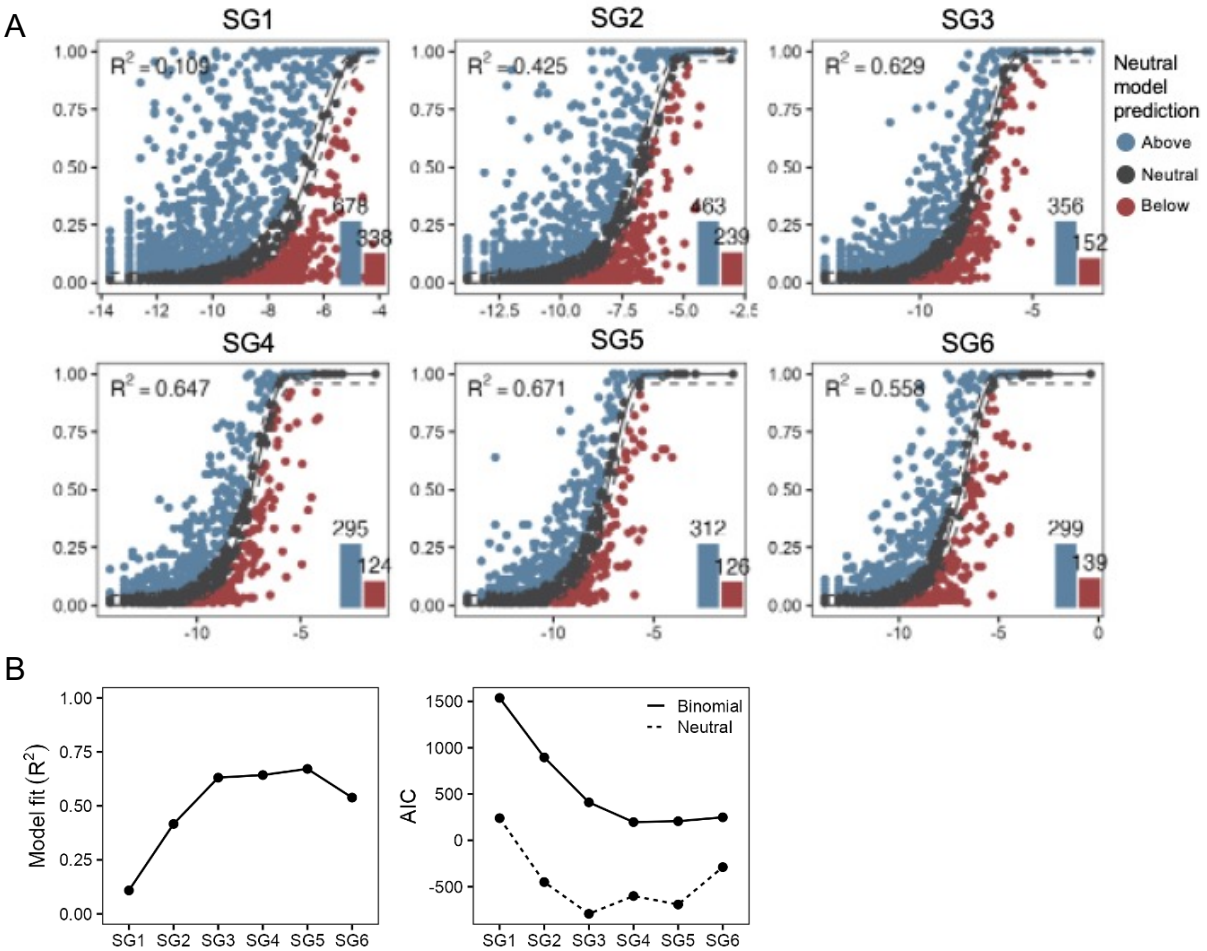

Supplemental Figure 7. Neutral community models for Rice Field selection line microbiomes at each selection generation. (**A**) We fit ASV relative abundance data to neutral models using the previous generation's community to parameterize migration and replacement rates. Gray points fall within the 95% confidence interval for abundance-occupancy values (x and y axes, respectively) expected if the community were assembled via neutral processes alone. Blue and red points indicate ASVs outside this prediction and therefore more likely experiencing positive and purifying selection, respectively. R-squared values for each plot indicate the overall model fit; blue and red bars in the bottom right corner of each plot show the total number of ASVs above and below neutral model predictions. (**B**) Given the improved fit of neutral models in later selection generations, neutral processes appear to become more important to microbiome assembly over time. Additionally, neutral models consistently outperformed binomial ones, which produced similar abundance-occupancy curves but without parameterization.

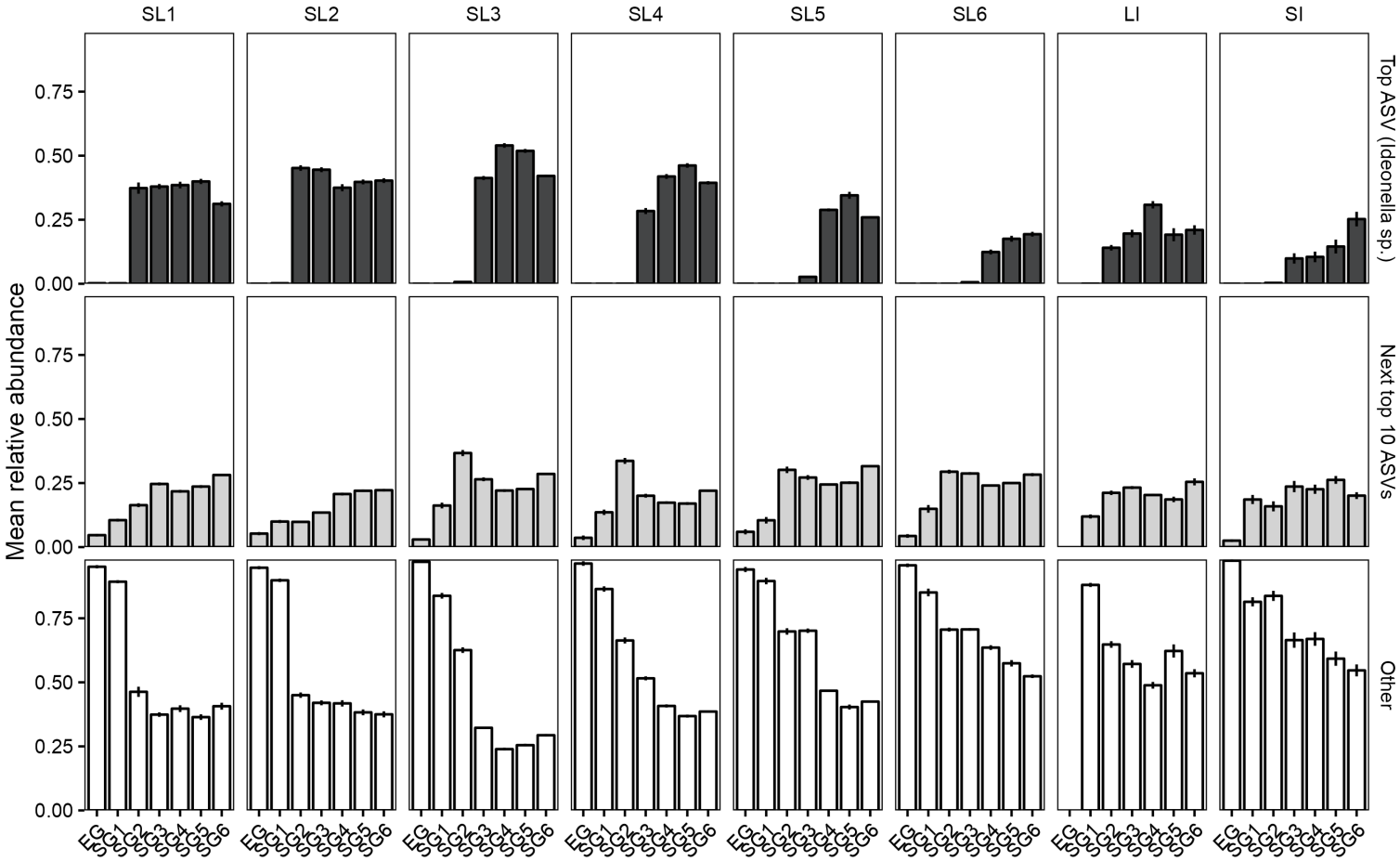

Supplemental Figure 8. Most abundant ASVs within Rice Field microbiomes. One ASV in particular—identified as belonging to the genus *Ideonella*—rose to high abundance in Rice Field microbiomes, sometimes accounting for more than 50% of the relative abundance of the community. Often, the combined relative abundance of next top ten most abundant taxa was still less than that of *Ideonella* sp. Regardless, both showed patterns of enrichment over time in all selection lines as well as sterile- and live-inoculated microbiomes. Bars represent mean relative abundance +/- one standard error.

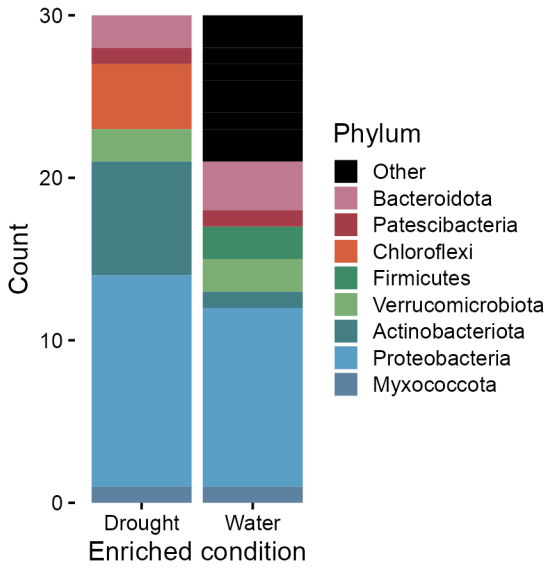

Supplemental Figure 9. ASVs identifies as significantly and consistently enriched in either selection line (drought) or live-inoculated (water) microbiomes. After filtering for FDR-corrected significant enrichment and an effect size greater than 0.5 (indicating significant and strong enrichment signal) we further subset to ASVs meeting these criteria in at least three selection generations. In total, 30 drought and 30 water indicators remained.

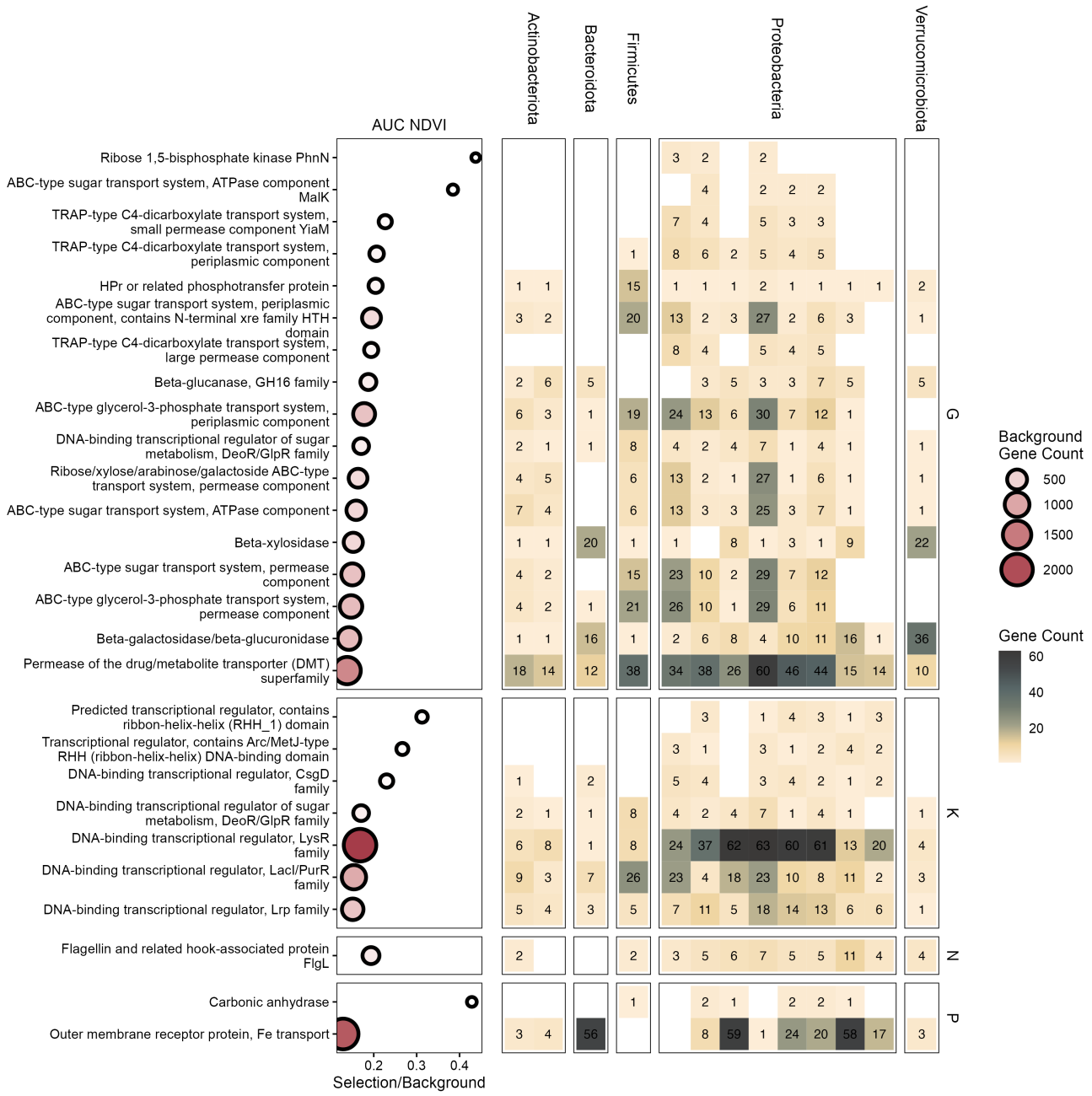

Supplemental Figure 10. Enrichments of individual COGs within significantly enriched categories associated with AUC NDVI balance numerator taxa. As in Figure 7, Selection/Background refers to the ratio of gene counts among phenotype-associated taxa relative to all taxa, but for individual COGs rather than COG functional categories. All COGs shown were significantly enriched in balance taxa, even after applying multiple testing corrections scaled by the total number of COGs within each functional category. Each column in the heatmap represents an individual MAG; columns are grouped by phylum. Numbers within heatmap cells indicate the COG gene count for each MAG.

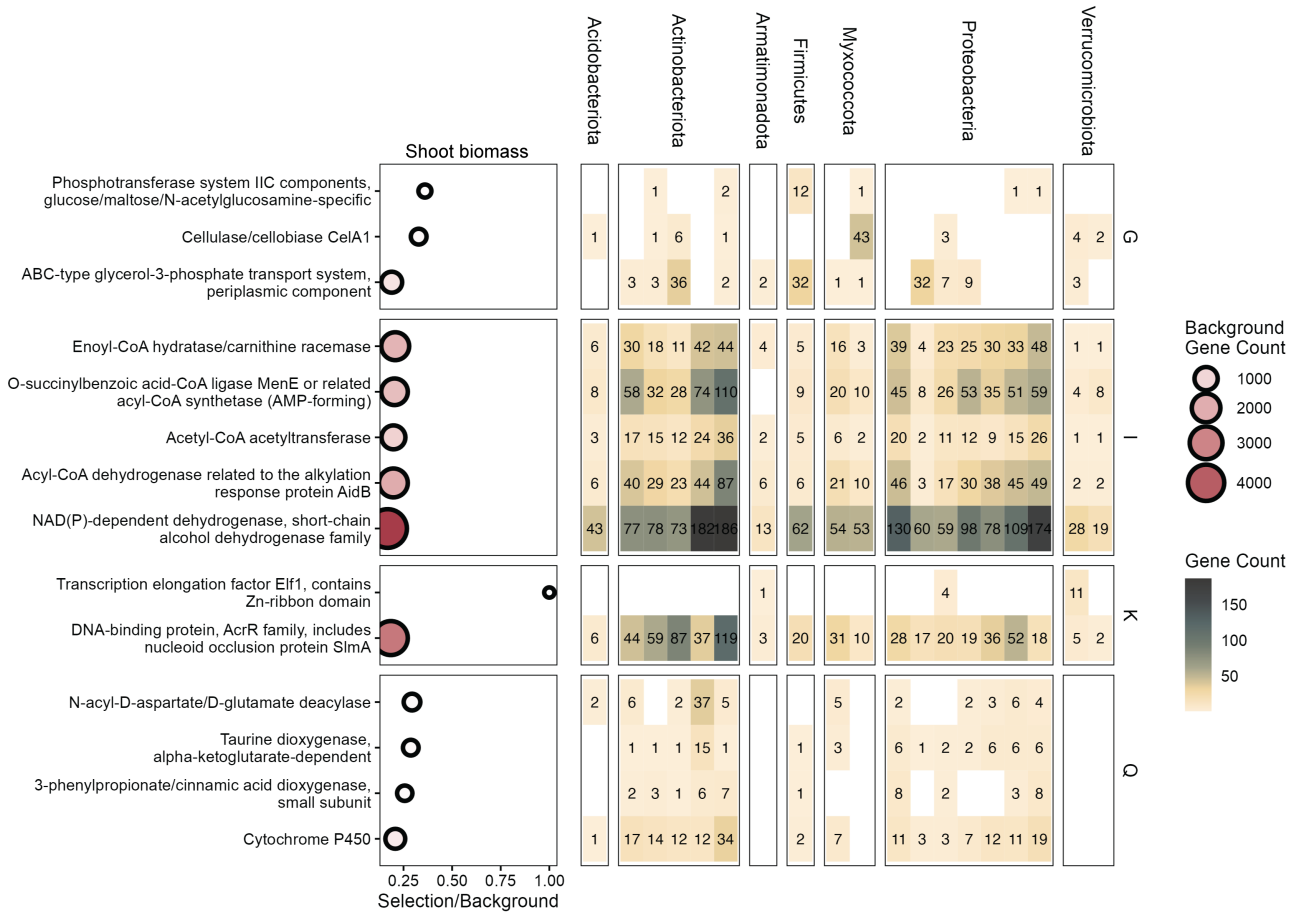

Supplemental Figure 11. Enrichments of individual COGs within significantly enriched categories associated with shoot biomass balance numerator taxa. As in Figure 7, Selection/Background refers to the ratio of gene counts among phenotype-associated taxa relative to all taxa, but for individual COGs rather than COG functional categories. All COGs shown were significantly enriched in balance taxa, even after applying multiple testing corrections scaled by the total number of COGs within each functional category. Each column in the heatmap represents an individual MAG; columns are grouped by phylum. Numbers within heatmap cells indicate the COG gene count for each MAG.

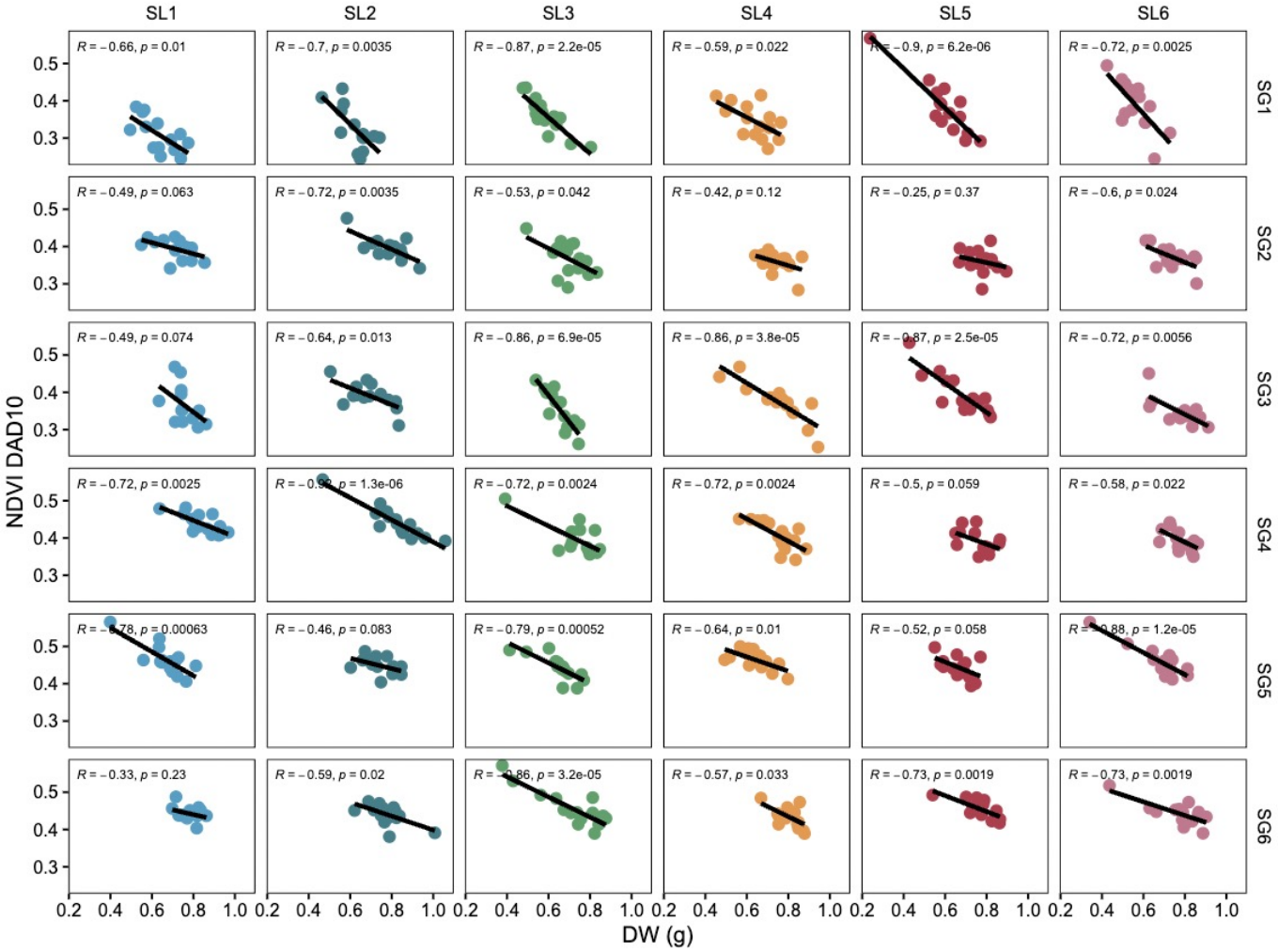

Supplemental Figure 12. NDVI values for plants at 10 days after drought (DAD 10) decrease as rice shoot dry weight biomass increases. Data shown here are for Rice Field selection line plants only, but this pattern held true for other soil treatments and SI plants as well.